John M. Louis*
Irene T. Weber†
József Tőzsér‡
G. Marius Clore*
Angela M. Gronenborn*

*Laboratory of Chemical Physics
National Institute of Diabetes
Digestive and Kidney Diseases
National Institutes of Health
Bethesda, Maryland 20892-0580
†Department of Microbiology and Immunology
Kimmel Cancer Center
Thomas Jefferson University
Philadelphia, Pennsylvania 19107
‡Department of Biochemistry and Molecular Biology
University Medical School of Debrecen
H-4012, Debrecen, Hungary

HIV-1 Protease: Maturation, Enzyme Specificity, and Drug Resistance

I. Introduction

Human immunodeficiency virus type 1 protease (HIV-1 PR) plays an indispensable role in the viral replication cycle. The PR catalyzes the hydrolysis of specific peptide bonds within the HIV-1 Gag and Gag-Pol polyproteins for its own maturation and to produce the other mature structural and functional proteins (Darke *et al.*, 1988; Oroszlan and Luftig, 1990). The active form of the 99-amino-acid-long mature PR is a homodimer. Optimal catalytic activity of the mature PR and ordered processing of the polyproteins are critical for the liberation of infective progeny virus (Oroszlan and Luftig, 1990; DeBouck, 1992; Kaplan *et al.*, 1993; Rose *et al.*, 1995). The initial critical step in the maturation reaction is the formation of an active PR dimer, formed from two Gag-Pol precursors, which is necessary for the release of the mature PR from the precursor. Furthermore, the cleavage at the N terminus of the PR is essential for the liberation of maturelike catalytic

Advances in Pharmacology, Volume 49

1054-3589/00 $35.00

activity (Louis *et al.*, 1994) and optimal ordered processing of Gag and viral infectivity (Tessmer and Krausslich, 1998). The level of expression of the Gag-Pol precursor relative to the Gag and the spatial arrangement of the PR domain within the Gag-Pol are also important (Krausslich, 1991). Overexpression of the Gag-Pol precursor results in intracellular activation of the PR and inhibition of virus assembly, suggesting that concentration-dependent dimer formation plays a key role in regulating the autocatalytic maturation of the PR in the viral life cycle (Karacostas *et al.*, 1993).

The mature PR has proven to be a most effective target for antiviral therapy of AIDS. However, the long-term potency of current PR inhibitors as therapeutic agents is limited by the rapid development of drug-resistant variants of the PR. Therefore it is critical to understand the molecular mechanisms of the proteolytic processes of the wild-type and drug-resistant mutants of PR in order to aid the development of new inhibitors and therapeutic strategies. Viral replication is limited by the relative activity of the PR for the sequential processing of the polyproteins. Up to 400-fold differences in the rates of hydrolysis were shown for different cleavage sites in Gag (Pettit *et al.*, 1994). Thus, it is critical to examine the drug-resistant mutant forms of the precursor and the mature enzyme for changes in the structural properties, kinetics, and specificity for natural substrates as compared to the wild-type enzyme.

In this article, we focus on three critical features of the HIV-1 PR, namely autocatalytic maturation from the precursor, substrate specificity, and emergence of drug resistance, utilizing protein and peptide design, enzyme kinetics, X-ray crystallography, and NMR spectroscopy.

II. Organization of the Gag-Pol Precursor and Molecular Structure of the Mature PR

The structural and functional proteins of retroviruses are produced through translation of polycistronic messenger RNAs into precursor proteins (Oroszlan and Luftig, 1990). In HIV-1, the Gag polyprotein consists of the structural proteins in the arrangement MA-CA-p2-NC-p1-p6 (Fig. 1 [Genbank: HIVHXB2CG]; Henderson *et al.*, 1992; Wondrak *et al.*, 1993). The Gag-Pol polyprotein is translated *via* a mechanism in which a -1 frameshift of an adenosine residue changes the open reading frame from Gag to Pol at a frequency of 5 to 10% (Jacks *et al.*, 1988; Hatfield *et al.*, 1992). This ribosomal frameshift site corresponds to the second codon within p1, leading to the synthesis of the transframe region (TFR or p6*), which links the structural Gag domain to the functional Pol domain (Fig. 1). Thus, the structure of Gag-Pol is MA-CA-p2-NC-TFR-PR-RT-IN (Fig. 1; Gorelick and Henderson 1994). A protease cleavage site separates each of the subdomains of the precursors.

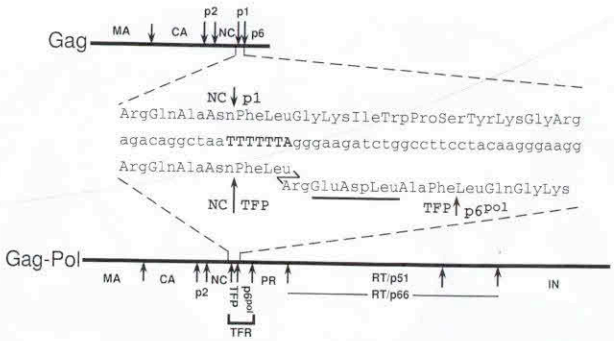

FIGURE 1 Structural organization of the Gag and Gag-Pol polyproteins of HIV-1 (bold lines). The nucleotide and protein sequence surrounding the translation frameshift site are shown. Arrows indicate the specific sites of cleavage by the viral PR. The DNA and encoded amino acids spanning the NC↓p1 junction in the Gag polyprotein and NC↓TFP and TFP↓$p6^{pol}$ junctions in the Gag-Pol polyprotein are aligned. Bold letters in the DNA sequence denote the conserved signal sequence required for ribosomal frameshifting. TFP denotes the eight conserved amino acids flanking NC. The remainder of the transframe region (TFR) constitutes $p6^{pol}$. The N-terminal dipeptide sequence of TFP is common with Gag p1. The second amino acid of TFP is either Leu or Phe at a ratio of ~7:3, which is dependent upon variation in the frameshifting mechanism and does not alter the remaining sequence of TFP. The underlined amino acid sequence represents the tripeptide core of TFP that inhibits the PR. The coding sequence for the tripeptide Glu-Asp-Leu corresponds to a region in the viral RNA between conserved regions of the signal sequence and the RNA secondary structure. Nomenclature of viral proteins is that of Leis *et al.* (1988).

Retroviral proteases including HIV-1 PR are 99–125 residues in size and contain the characteristic active site triad, Asp-Thr/Ser-Gly (amino acids 25–27 in HIV-1). They are enzymatically active as homodimers in acidic conditions and are structurally similar to pepsinlike proteases which function as monomers. In addition to the catalytic triad, retroviral proteases contain a second highly conserved region (Gly86-Arg87-Asn88 in HIV-1) that is not present in the cellular aspartic proteases (Pearl and Taylor, 1987; Copeland and Oroszlan, 1988). Even a conservative mutation of Arg87→Lys in this region renders the enzyme inactive (Louis *et al.*, 1989). Conserved regions of the PR are important for both catalysis and dimer formation (Weber, 1990; Gustchina and Weber, 1991). Crystal structures have been determined of HIV PR in the presence and absence of inhibitors (reviewed in Wlodawer and Erickson, 1993). The two chemically identical subunits of the PR dimer are in a nearly symmetric arrangement. Each subunit folds into a compact structure of β-strands with a short α-helix near the C terminus (Fig. 2). Residues 44–57 of each subunit form a pair of antiparallel β-strands called the flap. The β-turn at the tip of the flap contains conserved glycines. The flaps are flexible and are thought to fold down over the substrate or inhibitor and act during catalysis both to bind substrate and exclude water from the active site. Mutation of flap residues results in dramatic

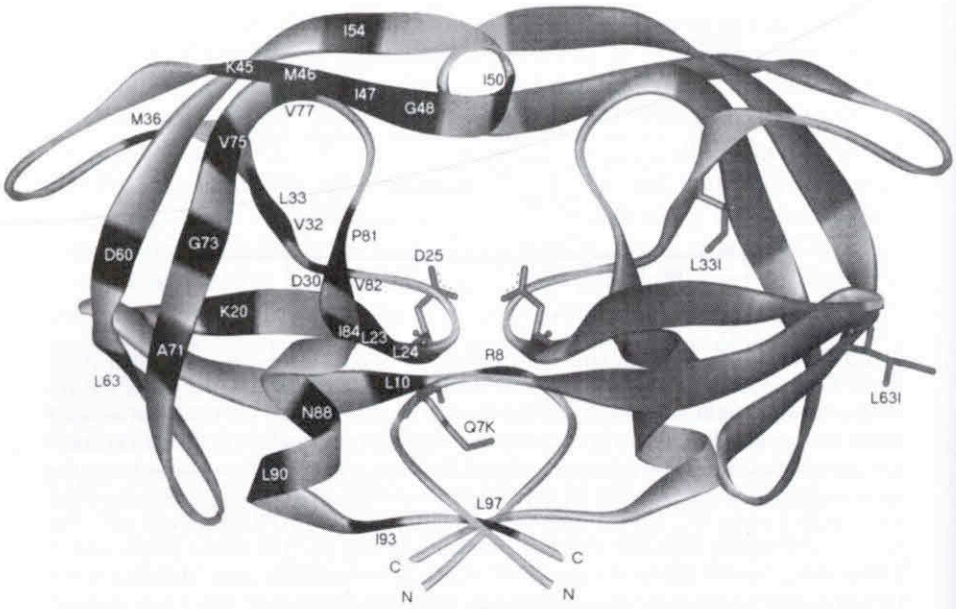

FIGURE 2 Crystal structure of HIV-1 PR. Shaded regions in one monomer indicate the secondary structure of the dimeric enzyme. The three mutations Q7K, L33I, and L63I in the PR to prevent its intrinsic autoproteolysis (degradation) and the active site aspartic acid residues of each monomer are shown in a stick representation. Positions of drug-resistant mutations are indicated in black.

reductions in enzyme activity (Tözsér *et al.*, 1997a). Intersubunit interactions are found between the two catalytic triads (Asp 25-Gly 27); Ile 50 and Gly 51 at the tip of the flaps; the complex salt bridge between Asp 29, Arg 87, and Arg 8′ from the other subunit; and the β-sheet formed by the four termini in the dimer (residues 1–4 and 96–99). These terminal residues form one half of the substrate sequence for cleavage at the $p6^{pol} \downarrow$ PR and PR $\downarrow$ RT junctions in the Gag-Pol precursor. The substrate binding site is formed by residues 8, 23–30, 32, 45–50, 53, 56, 76, 80–82, and 84. In addition, a number of other PR residues contribute to both the substrate binding and the interface contacts. These important regions are highly conserved in sequence among different isolates of HIV-1 (Gustchina and Weber, 1991) and retroviral proteases share similar structures in these regions (Weber, 1990; Wlodawer and Erickson, 1993).

III. Mechanism and Regulation of PR Maturation

PR-mediated processing of Gag and Gag-Pol and particle maturation are complex events (Vogt, 1996). The TFR, which flanks the N terminus

of PR in Gag-Pol (see Fig. 1), is thought to have a role similar to that observed at the N termini of zymogen forms of cellular aspartic proteases. In accordance, early studies have demonstrated that a deletion of the TFR domain leads to a significantly higher rate of processing activity of the Gag-ΔPol precursor, suggesting that TFR negatively regulates PR function (Partin *et al.*, 1991). TFR consists of two domains, the N-terminal transframe octapeptide (TFP), which is conserved in all variants of HIV-1, and a 48- to 60-amino-acid variable region $p6^{pol}$ (Gorelick and Henderson, 1994; Candotti *et al.*, 1994; Louis *et al.*, 1998). TFP and $p6^{pol}$ are separated by a PR cleavage site (Phylip *et al.*, 1992; Louis *et al.*, 1999a). An isolated 68-amino-acid TFR has no overall stable secondary or tertiary structure, although a small potential for helix formation at its N terminus was shown by NMR (Beissinger *et al.*, 1996).

A. Kinetics and Mechanism of Autoprocessing of a Model Precursor

Since kinetic studies to understand the mechanism of the autocatalytic maturation reaction of the full-length Gag-Pol polyprotein are difficult to perform due to the presence of at least nine PR cleavage sites (Fig. 1), a model PR precursor that contains only the two cleavage sites flanking the PR domain was developed. This model polyprotein (MBP-Δ$p6^{pol}$-PR-ΔRT; Fig. 3) was constructed by adding 19 residues of the native reverse transcript-

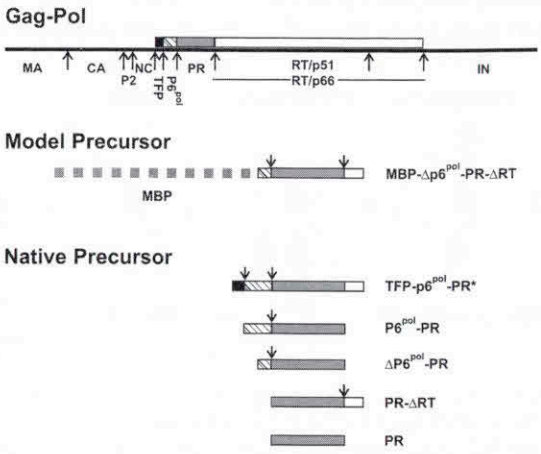

FIGURE 3 Model and native precursor constructs of the PR. The Gag-Pol polyprotein of HIV-1 is shown on top (see legend to Fig. 1). The domains TFP, $p6^{pol}$, and RT flanking the PR (gray) are shown as closed, hatched, and open boxes, respectively. The dashed gray line denotes the 38-kDa maltose-binding protein (MBP). The catalytic activities of MBP-Δ$p6^{pol}$-PR-ΔRT (referred to as MBP-ΔTF-PR-ΔPol in Louis *et al.*, 1994), TFP-$p6^{pol}$-PR*, $p6^{pol}$-PR, and Δ$p6^{pol}$-PR are significantly lower relative to that of the PR-ΔRT and mature PR.

ase sequence (ΔRT) to the C terminus of the PR domain and 12 residues of the native $p6^{pol}$ region ($\Delta p6^{pol}$) to its N terminus, which was additionally fused to the maltose binding protein (MBP) of *Escherichia coli* (Louis *et al.*, 1991a). Aggregation of the precursor upon its expression in *E. coli* allowed its isolation in an intact form. Upon refolding the protein from 8 *M* urea, the model precursor undergoes time-dependent autoprocessing to release the mature PR in two consecutive steps. Initial mutational studies of the cleavage sites in the model polyprotein showed that the N-terminal cleavage is more sensitive to mutations and that it precedes the cleavage at the C terminus of the PR (Louis *et al.*, 1991a,b). Investigation of the time-dependent autocatalytic maturation of MBP-$\Delta p6^{pol}$-PR-ΔRT by kinetics led to the mechanism summarized in Fig. 4 (Louis *et al.*, 1994).

1. Processing of the N-Terminal Strands Is Intramolecular

In the mechanism illustrated in Fig. 4, the full-length precursor dimerizes to form tetrapod 1. The dimeric protein binds inhibitors and substrates in a similar manner to the mature enzyme, although its enzymatic activity is significantly lower than that of the mature PR. For autoprocessing to occur, tetrapod 1, which is not an obligatory intermediate, undergoes a conformational change to tetrapod 2, in which one of the two N-terminal strands occupies its active site. Cleavage of the scissile peptide bond at the N terminus is the rate-determining step for the appearance of enzymatic activity. The bipod (PR-ΔRT, see Figs. 3 and 4), which is converted relatively slowly to the mature PR, has catalytic activity comparable to that of the mature enzyme. Restricting the cleavage at the $p6^{pol} \downarrow$ PR site in the model precursor leads to reduced cleavage at the C terminus of PR (Louis *et al.*, 1991b). *In*

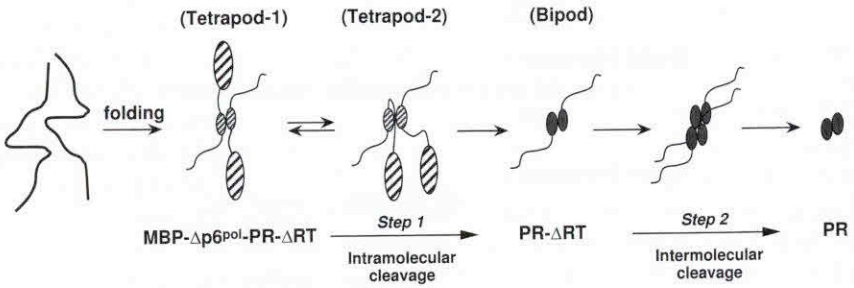

FIGURE 4 Proposed mechanism for the autocatalytic maturation of the HIV-1 PR from the model polyprotein MBP-$\Delta p6^{pol}$-PR-ΔRT. The MBP and PR are denoted as large hatched ovals and small hatched ovals, respectively. Lines represent $\Delta p6^{pol}$ and ΔRT sequences that flank the PR domain. The PR catalyzes the hydrolysis of its N terminus from a transiently dimeric MBP-$\Delta p6^{pol}$-PR-ΔRT *via* an intramolecular mechanism to release the intermediate PR-ΔRT (Step 1). Subsequent conversion of the PR-ΔRT (bipod) to the mature PR occurs *via* an intermolecular mechanism (Step 2). The two conformational isomers of the dimeric MBP-$\Delta p6^{pol}$-PR-ΔRT are referred to as Tetrapods 1 and 2. Hatched ovals of the PR domain denote the low catalytic activity of the PR precursor as compared to the bipod and mature PR.

vivo, a blocking mutation at the $p6^{pol} \downarrow$ PR site in the Gag-Pol precursor allows maturation of PR to occur at the native TFP $\downarrow p6^{pol}$ and PR $\downarrow$ RT sites to release a $p6^{pol}$–PR intermediate, which, however, is defective in Gag processing and viral infectivity (Tessmer and Krausslich, 1998).

A similar mechanism for the processing of the PR at its N terminus has been proposed in studies using a mini-precursor in which a mutated PR (Ala28→Ser) was fused to 25 amino acids of the native $p6^{pol}$ sequence ($\Delta p6^{pol}$-$PR^{Ala28 \rightarrow Ser}$; Co *et al.*, 1994). The mutation Ala28→Ser in the mature PR lowers the k_{cat}/K_m by about 250-fold relative to the wild-type mature PR and thus permitted the isolation of the precursor upon its expression in *E. coli* (Ido *et al.*, 1991). This mini-precursor reportedly undergoes time-dependent maturation but with no significant change in the catalytic activity, contrary to our results using the model construct. The proposed mechanism for the maturation of the HIV-1 PR at its N terminus is strikingly similar to that observed for the conversion of pepsinogen to pepsin, a monomeric mammalian aspartic acid protease (Louis *et al.*, 1994).

2. *Processing of the C-Terminal Strands Is Intermolecular*

Unlike the C terminus of pepsinogen, which is not modified during the activation process, the C terminus of the HIV-1 PR precursor is processed to generate the mature PR. The kinetic order of the reaction involving the bipod monomer (PR-ΔRT, see Fig. 3; Wondrak *et al.*, 1996) was determined by following the initial rates of the reaction. A linear relationship between the rate of conversion (disappearance of the bipod and the appearance of the mature PR) and the square of the protein concentration (varied over sevenfold) indicates that the reaction is bimolecular (intermolecular). Unlike the MBP-$\Delta p6^{pol}$-PR-ΔRT, which has very low catalytic activity, both the kinetic parameters for the hydrolysis of the peptide substrate catalyzed by the PR–ΔRT and the inhibition constant determined with a pseudopeptide inhibitor are indistinguishable from those determined for the mature enzyme. In addition, the pH profile for k_{cat}/K_m is similar to that of the mature PR. Activity of the bipod or change in the intrinsic protein fluorescence, both monitored as a function of enzyme dilution, indicated that the majority of the bipod is in the dimeric form under the protein concentrations employed in the kinetic studies.

Our results show that the model precursor exhibits very low catalytic activity prior to the cleavage at the $p6^{pol} \downarrow$ PR junction, the N terminus of PR. In contrast, several mutated PR fusion proteins that either contain a mutation at the $p6^{pol} \downarrow$ PR junction or contain short native or nonnative sequences flanking the N terminus of PR were shown to exhibit catalytic activities comparable to that of the wild-type mature PR (Vogt, 1996; Wondrak and Louis, 1996). This raised the question whether the MBP in our model construct impeded PR folding/dimerization, catalytic activity, and/or the observed kinetics of the maturation reaction. Therefore the auto-

processing reaction was also analyzed using a PR precursor linked to the native transframe region containing the native cleavage sites as described in the next section.

B. Kinetics of Maturation of Native Precursors

1. Maturation of p6^{pol}-PR Precursor

A native p6^{pol}-PR precursor (see Figs. 1 and 3) containing a native cleavage site at the p6^{pol} ↓ PR junction was expressed and purified. To circumvent aggregation of the precursor associated with Cys thiol oxidation that may lead to anomalous kinetic measurements of the autoprocessing reaction, Cys residues 67 and 95 in the PR were replaced with Ala. These mutations do not alter the kinetic parameters or the structural stability of the mature mutant enzyme (Louis *et al.*, 1999a). The renatured p6^{pol}-PR undergoes a time-dependent maturation reaction concomitant with a large increase in enzymatic activity similar to that of the model precursor (Fig. 5). At ≥pH 5.0, the reaction proceeds in a single step to produce the mature enzyme, whereas at pH <5.0 it is characterized by the appearance and disappearance of a single protein intermediate that migrates between p6^{pol}-PR and PR bands (indicated by arrow in Figs. 5 and 6; see Louis *et al.*, 1999a). This intermediate (termed Δp6^{pol}-PR) is generated via cleavage at the Leu24 ↓-Gln25 site within p6^{pol} (Fig. 3; Zybarth *et al.*, 1994; Louis *et al.*, 1999a).

The formation of these intermediate precursors under suboptimal conditions for the autoprocessing reaction is similar to that observed for the conversion of the zymogen form of the gastric protease pepsin, which, unlike retroviral proteases, is a monomeric enzyme (Khan and James, 1998). The zymogen pepsinogen differs from mature pepsin by a 44-amino-acid-long positively charged N-terminal proregion. Below pH 2.0, pepsinogen is converted in a single step through an intramolecular maturation process to pepsin with a homogenous N terminus, whereas at pH 4.0 the activation product is heterogeneous with multiple N-terminal products (al-Janabi *et al.*, 1972).

The maturation reaction of p6^{pol}-PR displays good first-order kinetics similar to those of the model precursor between pH 4.0 and pH 6.5, as indicated by a linear relation between the rate of increase in maturelike catalytic activity and protein concentration (inset Fig. 5). Plots of the measured densities corresponding to the starting material and the product (mature PR) and the rate of increase in maturelike catalytic activity versus time are shown superimposed on each other (Fig. 5). The first-order rate constants for the maturation reaction of p6^{pol}-PR and MBP-Δp6^{pol}-PR-ΔPR are similar (Louis *et al.*, 1999a). The first-order rate constant displays a bell-shaped dependency on pH with two ionizable groups having pK_as of 4.9 and 5.1 (Louis *et al.*, 1999a). This pH profile is quite similar to that obtained for the maturation of the mini-precursor Δp6^{pol}-PR$^{Ala28 \rightarrow Ser}$ (Co *et al.*, 1994).

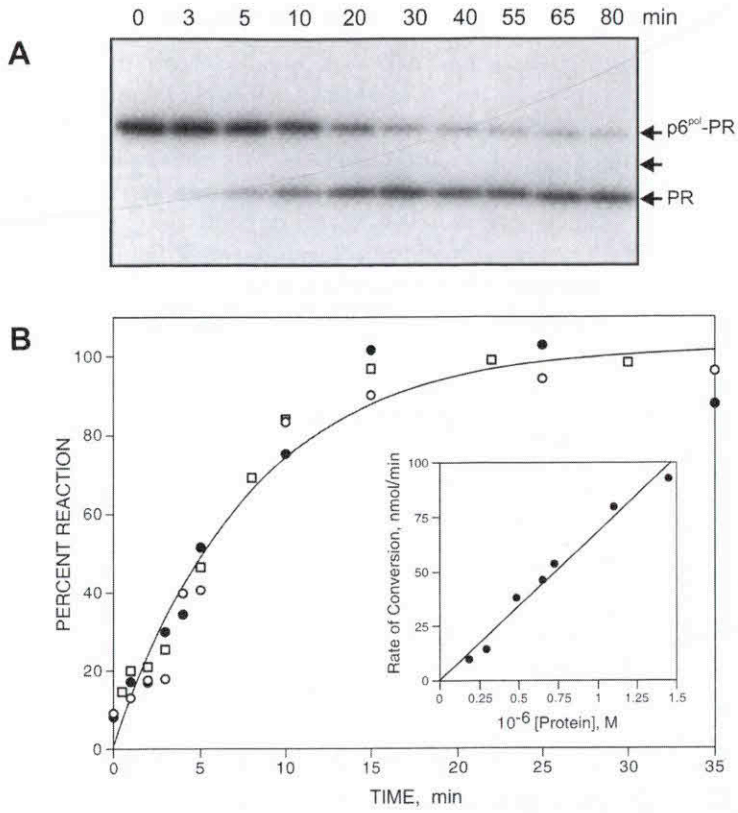

FIGURE 5 (A) Time course of the autocatalytic maturation of $p6^{pol}$-PR at pH 5.8 in 50 m*M* sodium acetate at 25°C. Aliquots of the reaction mixture were drawn at the desired time and subjected to 10–20% SDS–PAGE and immunoblotting. The relative mobilities of the full-length precursor and mature PR are indicated by arrows. Band intensities were quantified by densitometry. (B) Time course of the reaction measured by following the increase in enzymatic activity (□), appearance of PR (●), and disappearance of $p6^{pol}$-PR (○) at pH 4.8. Inset in B is a plot of the dependence of the initial rate of the reaction measured by following the increase in enzymatic activity upon varying the protein concentration. The first-order rate constant measured by following the appearance of enzymatic activity for the maturation of $p6^{pol}$-PR under the same conditions as described for the model precursor are similar (Louis *et al.*, 1994, 1999a).

The higher pK_a of 5.1 observed for the maturation reaction is in agreement with the pK_a values of 4.8 and 5.2 obtained for the mature PR (Polgar *et al.*, 1994) and PR-ΔPol (Wondrak *et al.*, 1996), respectively, and for those reported using other fusion proteins of the PR (Wondrak and Louis, 1996). The lower pK_a of 4.9 observed for the maturation reaction is about 1.8 pH units higher than that observed for the wild-type mature PR (Polgar *et al.*, 1994).

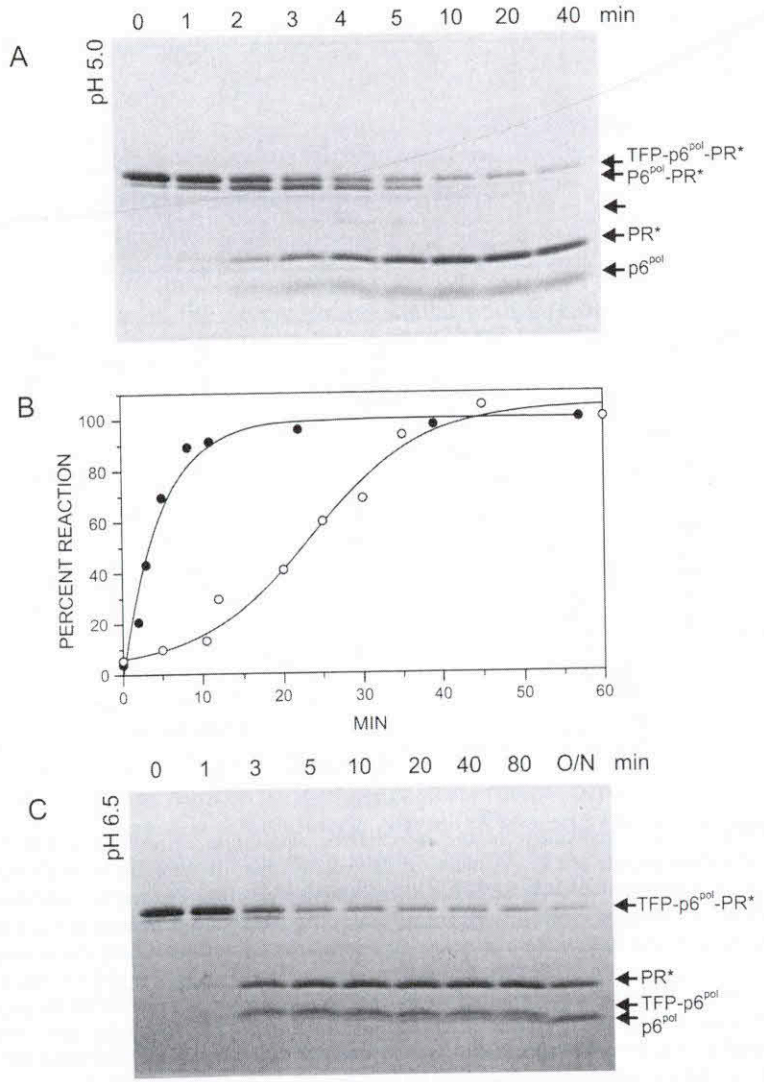

FIGURE 6 Time course of the autocatalytic maturation of TFP-p6^{pol}-PR* at pH 5.0 in 50 m*M* sodium formate, 0.5 *M* urea (A), and at pH 6.5 in 25 m*M* sodium phosphate (C) buffers. Aliquots of the reaction mixture were drawn at the desired time and subjected to 10–20% SDS–PAGE in Tris–Tricine buffer. Protein bands were visualized by Coommasie brilliant G250 staining. The relative mobilities of the full-length precursor and product peaks are indicated by arrows. (B) The time course of the autoprocessing of TFP-p6^{pol}-PR* monitored by following the appearance in enzymatic activity at pH 4.0 (●) and pH 6.5 (○). The lag in the reaction time course coincides to the accumulation of the transient intermediate p6^{pol}-PR* (see A) that is subsequently converted to the mature PR*.

2. *Maturation of TFP-p6^{pol}-PR* Precursor*

To conduct structural studies of the PR precursor fused to the intact transframe region (TFP-p6^{pol}), a construct which spans the Gag-Pol sequence starting from the NC ↓ TFP junction and ending with the C-terminal amino acid of the PR was expressed (see Figs. 1 and 3). The PR domain in this TFP-p6^{pol}-PR* construct bears the following mutations, Gln7→Lys, Leu33→Ile, Leu63→Ile, Cys67→Ala, and Cys95→A, designed to limit autoprotolysis (degradation of PR) and to prevent Cys thiol oxidation. Importantly, these five mutations do not alter the kinetics or the structural stability of the mature PR* as compared to that of the wild-type mature PR (Rose *et al.*, 1993; Mildner *et al.*, 1994; Mahalingam *et al.*, 1999; Louis *et al.*, 1999a,b). However, the accumulation of a small fraction of the full-length precursor (<5% of the total expressed protein) permitted its purification in just sufficient amounts for kinetic analyses (Louis *et al.*, 1999b).

The full-length precursor TFP-p6^{pol}-PR* has two known native PR cleavage sites, TFP ↓ p6^{pol} and p6^{pol} ↓ PR (Figs. 1 and 3). Since PR-catalyzed hydrolysis of peptides with amino acid sequences corresponding to the two cleavage sites, TFP ↓ p6^{pol} and p6^{pol} ↓ PR, have comparable kinetic parameters (Phylip *et al.*, 1992; Louis *et al.*, 1998), we anticipated complex kinetics and multiple products for the maturation of the PR from TFP-p6^{pol}-PR*. In contrast, TFP-p6^{pol}-PR* undergoes an ordered two-step maturation reaction (Fig. 6A). At pH 5, the first step involves the cleavage of the peptide bond at the TFP/p6^{pol} site to produce the transient intermediate p6^{pol}-PR, which is subsequently converted to the mature PR*. A plot of the rate of appearance of enzymatic activity *versus* time is characterized by a lag period followed by a first-order process indicating that (1) TFP-p6^{pol}-PR* has the same low catalytic activity as that of the intermediate precursor p6^{pol}-PR* and (2) cleavage at the N terminus of the PR (p6^{pol} ↓ PR site) is concomitant with the appearance of maturelike catalytic activity (Fig. 6B). Following the reaction at pH 6.5 no lag period is observed due to preferential cleavage at the p6^{pol} ↓ PR site which precedes that of the TFP ↓ p6^{pol} site releasing the mature PR* (Figs. 6B and 6C).

C. TFP, a Hydrophlic Competitive Inhibitor of the Mature PR

TFP, the N terminus of TFR, may have a regulatory role for the autoprocessing of the PR from the Gag-Pol precursor *in vivo*. TFP and its analogs are competitive inhibitors of the mature PR (Fig. 7A; Louis *et al.*, 1998). The smallest and most potent of the analogs are tripeptides Glu-Asp-Leu and Glu-Asp-Phe with K_is of ca. 50 and 20 μM, respectively. Other substitutions or deletions in the tripeptide Glu-Asp-Leu lead to higher K_is. Substitution of the acidic amino acids in the TFP by neutral amino acids and D- or retro-D configuration of Glu-Asp-Leu results in a >40-fold increase in K_i.

A

PEPTIDE	K_i, μM
Phe-Leu-Arg-Glu-Asp-Leu-Ala-Phe	98 ± 10
Phe-Leu-Arg-Gln-Asn-Leu-Ala-Phe	>2000
Glu-Asp-Leu-Ala	160 ± 20
Glu-Asp-Leu	50 ± 9
Arg-Glu-Asp	3360 ± 400
Glu-Asn-Leu	3070 ± 210
Glu-Asp-Phe	25 ± 3

B

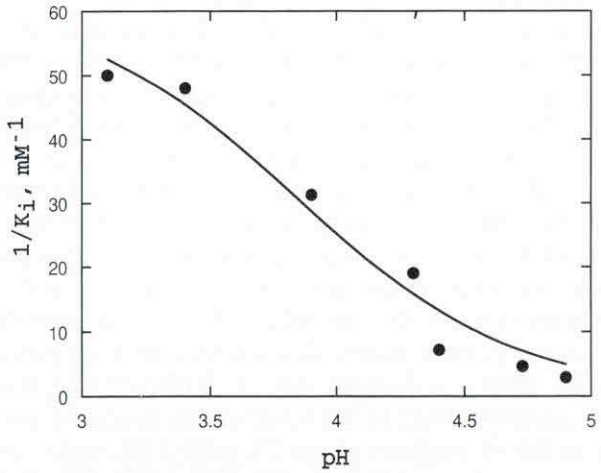

FIGURE 7 The hydrophilic TFP is a specific competitive inhibitor of the mature HIV-1 PR. (A) Inhibition of the action of HIV-1 PR by TFP Phe-Leu-Arg-Glu-Asp-Leu-Ala-Phe and its analogs. The K_i was obtained from a plot of the apparent K_m vs [I] for peptides or from a plot of $1/V$ *vs* [I] at saturating concentration of the substrate. Assays were performed in 50 m*M* sodium formate at pH 4.25 and 2.5 m*M* DTT. The final enzyme and substrate concentrations were 150 n*M* and 390 μM, respectively. All amino acids are of the L-configuration. (B) A plot of inhibition (K_i) by Glu-Asp-Leu for PR-catalyzed hydrolysis of substrate Lys-Ala-Arg-Val-Nle-Phe(NO_2)-Glu-Ala-Nle-NH_2 vs pH. The K_is were obtained from plots of $1/V$ versus [I] at a saturating concentration of the substrate (390 μM). Reactions were carried out in 50 m*M* sodium formate or 100 m*M* sodium acetate buffers containing 2.5 m*M* DTT and 150 n*M* of PR at 25°C. The line is a calculated curve with a pK_a of 3.8 and a K_i of 20 μM.

Unlike other known inhibitors of the HIV-1 PR which are highly hydrophobic, Glu-Asp-Leu is extremely soluble in water and its binding affinity to the active site of the PR is not enhanced by increasing NaCl concentration. Inhibition of the PR by Glu-Asp-Leu is dependent on the protonated form

of a group with a pK_a of 3.8 (Fig. 7B). This result complements the observation of the stepwise maturation of TFP-p6^{pol}-PR* at different pH values. Decreasing pH leads to a higher affinity of TFP to the active site of the PR, promoting the processing at the TFP↓p6^{pol} site prior to the p6^{pol}↓PR site. It was not feasible to investigate the interaction of intact TFP with the PR under conditions of crystal growth due to its hydrolysis, giving rise to two products, Phe-Leu-Arg-Glu-Asp and Leu-Ala-Phe. But the interaction of the tripeptide core of TFP, Glu-Asp-Leu, as studied by X-ray crystallography is similar to those of other product–enzyme complexes (Louis *et al.*, 1998; Rose *et al.*, 1996). Similarly, peptides derived from the proregion of pepsinogen and prorenin have been shown to act as competitive inhibitors of mature pepsin and renin, respectively (Dunn *et al.*, 1978; Richards *et al.*, 1992).

D. Influence of Flanking Sequences on the Structural Stability of Protease Precursors

Loss in enzymatic activity of the mature PR correlates to loss of stable tertiary structure with increasing urea concentration (Wondrak *et al.*, 1996; Wondrak and Louis, 1996). The dimeric form of p6^{pol}-PR, which is mandatory for the formation of an active site capable of supporting a hydrolytic reaction, is highly sensitive to urea denaturation compared to the mature enzyme, which suggests that p6^{pol}-PR is structurally less stable than the mature PR (Louis *et al.*, 1999a). This result is in agreement with earlier studies showing that the PR domain, when fused to the 19 amino acids of the flanking C-terminal RT sequence (PR-ΔRT) or the short native or nonnative sequences at its N terminus, is also less stable toward urea denaturation (Wondrak *et al.*, 1996; Wondrak and Louis, 1996). The above results are also consistent with results showing that the mature PR is largely dimeric above 10 n*M* (Wondrak *et al.*, 1996), whereas inactive N-terminally extended forms of the PR linked to the TFR fail to dimerize in a qualitative assay (Zybarth and Carter, 1995).

Dissociation of the dimeric form of the mature PR* (autoproteolysis resistant) was also measured by following enzymatic activity as a function of enzyme dilution. Mature PR* exhibits a K_d <5 n*M* at pH 5.0, similar to that observed for the mature wild-type PR under identical conditions (Louis *et al.*, 1999b). Since TFP-p6^{pol}-PR* precursor undergoes cleavage at the p6^{pol} ↓ PR site as the first step at pH 6.5 (Figs. 6B and 6C), unlike at more acidic pH values, the simultaneous appearance of the maturelike enzymatic activity and the mature PR* protein product was used to evaluate the ability of TFP-p6^{pol}-PR* to undergo dimerization and autocatalytic maturation as a function of precursor concentration. A plot of specific enzymatic activity versus precursor concentration shows that the apparent K_d for TFP-p6^{pol}-PR* is ~680 n*M* (Louis *et al.*, 1999b). The decreased stability to urea and >130-fold increase in the apparent K_d of TFP-p6^{pol}-PR* as compared to

the mature PR* indicates that the structural stability of the PR domain is significantly lower in the precursor.

E. ^{1}H-^{15}N Correlation Spectra of Uniformly Labeled Precursor and Mature Proteases

The fact that the maturation reaction of the TFP-p6^{pol}-PR* and p6^{pol}-PR precursors can be monitored by following the increase in enzymatic activity is clear evidence that there is a large difference between the catalytic activity of the mature PR and that of PR precursor. The low catalytic activity seems to be intrinsic to the PR when linked to the native TFR with the native cleavage sites. This low catalytic activity could be either due to a conformational difference of the dimeric precursor that does not support efficient catalysis or could be an apparent effect of the equilibrium that largely favors the unfolded or partially folded form of the protein relative to the folded enzymatically active dimer. To analyze the PR precursor by NMR requires attaining sufficient quantity of the protein.

In other studies, inhibitor-resistant mutants of the PR fused to the intact TFR were expressed with the aim of understanding the relationship between PR maturation and drug resistance. One among several of these mutants that were analyzed for expression shows elevated level of precursor accumulation as compared to the construct TFP-p6^{pol}-PR*. We chose the R8Q mutant precursor (termed TFP-p6^{pol}-PR*^{Q}) as a good source for preparing sufficient amounts of precursor. Although the mature PR*^{Q} is more sensitive toward urea denaturation than PR*, the dissociation constant (K_d) and kinetic parameters for mature PR*^{Q}-catalyzed hydrolysis of the peptide substrate and the inhibition constant for the hydrolytic reaction with inhibitor are comparable to that of the wild-type PR and PR* (Mahalingham *et al.*, 1999; Louis *et al.*, 1999b). TFP-p6^{pol}-PR*^{Q} undergoes maturation to release the mature PR*^{Q}, similar in kinetics to that of the TFP-p6^{pol}-PR* precursor. We therefore employed uniformly ^{15}N-labeled TFP-p6^{pol}-PR*^{Q} precursor in our subsequent studies of HIV-1 PR maturation.

It appears that for HIV-1 PR, and possibly other viral aspartic proteases, activation is tightly coupled to folding. This is in contrast to most zymogens and their corresponding mature enzymes in which the catalytic machinery is stably preformed and activation is achieved by a conformational change after peptide bond cleavage which involves removing parts of the polypeptide chain protruding into or obstructing access to the active site. The TFP-p6^{pol}-PR precursor protein largely possesses all the hallmarks of an unfolded polypeptide chain and the ^{1}H-^{15}N correlation spectrum of uniformly labeled TFP-p6^{pol}-PR*^{Q} precursor protein at pH 5.0 presented in Fig. 8A exhibits the typical narrow shift dispersion observed for random-coil peptides or proteins (Wishart *et al.*, 1995). This is true for precursor protein in the absence or presence of any tight binding inhibitors. Cleavage at the p6^{pol}/

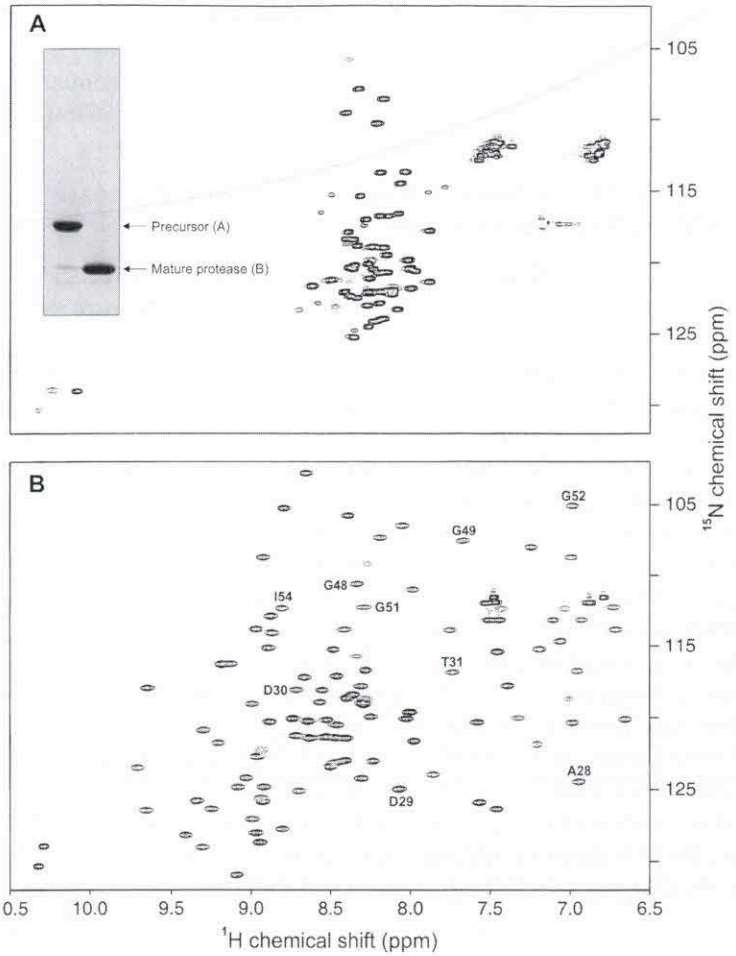

FIGURE 8 ^{1}H-^{15}N correlation spectra of the precursor TFP-p6^{pol}-PR*^{Q} and mature PR*^{Q} proteases in complex with 10-fold excess of DMP323 in 50 m*M* sodium acetate buffer, pH 5.2, at 25°C. (Inset) An aliquot of the sample was subjected to 20% SDS–PAGE and stained with Coomassie brilliant blue G250. There were no degradation products observed in both preparations but for a minor mature PR product released from TFP-p6^{pol}-PR*^{Q} that occurs at the protein-folding step even in the presence of excess inhibitor DMP 323.

PR site is concomitant with the appearance of stable tertiary structure and enzymatic activity. Figure 8B shows the corresponding ^{1}H-^{15}N correlation spectrum of the mature PR*^{Q} PR complexed with the symmetric tight binding inhibitor DMP323 (Lam *et al.*, 1994), demonstrating a stable three-dimensional structure. A comparison of chemical shifts observed for this mutant complex with previously reported data (Yamazaki *et al.*, 1994) reveals that the structure of the PR*^{Q} is extremely similar to that determined

for the wild-type mature enzyme. Viewed in the greater context of zymogen activation, the HIV-1 PR may represent the most extreme case of activation by conformational rearrangement, namely the transition from an unstructured, inactive precursor protein to a stably folded, active mature enzyme.

F. Plausible Mechanism of Regulation of the Protease in the Viral Replication Cycle

The results of studies using different model and native precursor proteins of the HIV-1 PR suggest that in HIV-1 and related retroviruses with similar organization of the Gag-Pol precursor, the transframe region flanking the N terminus of the PR may function as a negative regulator for protein folding and dimerization. The low dimer stability of the PR precursor relative to that of the mature enzyme is an ideal way of preventing enzymatic activity from emerging until the assembly of the viral particle is complete. Depending on the pH of the environment in which Gag-Pol maturation takes place, removal of the transframe region can either occur in two sequential steps or in a single step. Intramolecular cleavage at the $p6^{pol}$/PR site to release a free N terminus of PR is critical for the formation of a stable tertiary structure of the PR and enzymatic activity (Louis *et al.*, 1999b). Subsequent processing of the other Gag-Pol cleavage sites will occur rapidly via intermolecular processes. Contrary to the TFR, the RT domain flanking the C terminus of PR does not seem to influence the catalytic activity of the PR (Wondrak *et al.*, 1996; Cherry *et al.*, 1998). The Leu5/Trp6 cleavage within PR could be viewed as a final step in the PR-associated cascade of events, resulting in destabilization of the tertiary structure and promoting dissociation of the dimer, thereby down-regulating the catalytic activity of the PR in the viral life cycle (Rose *et al.*, 1993; Louis *et al.*, 1999b).

IV. Substrate/Inhibitor Interactions

Important conserved features of PR–inhibitor interactions have been identified by analysis of crystal structures (Gustchina *et al.*, 1994; Gustchina and Weber, 1991). This information is critical for the design of high-affinity PR inhibitors. Most inhibitors resemble peptides with the scissile peptide bond replaced by a nonhydrolyzable bond, such as the transition-state analogs containing a hydroxyl group instead of the peptide carbonyl oxygen. The PR interactions with peptidelike inhibitors are expected to resemble the interactions with the natural substrates (Fig. 9). Residues 8, 23–32, 45–56, 76, and 80–84 from both subunits form the binding site. About seven residues (P4 to P3′) of peptidelike inhibitors are bound between the catalytic aspartic acids and the two flexible flaps (Gustchina and Weber, 1991). The inhibitor is bound in an extended conformation and forms two short β-sheets with residues 25–29 and flap residues 48–50 from both subunits.

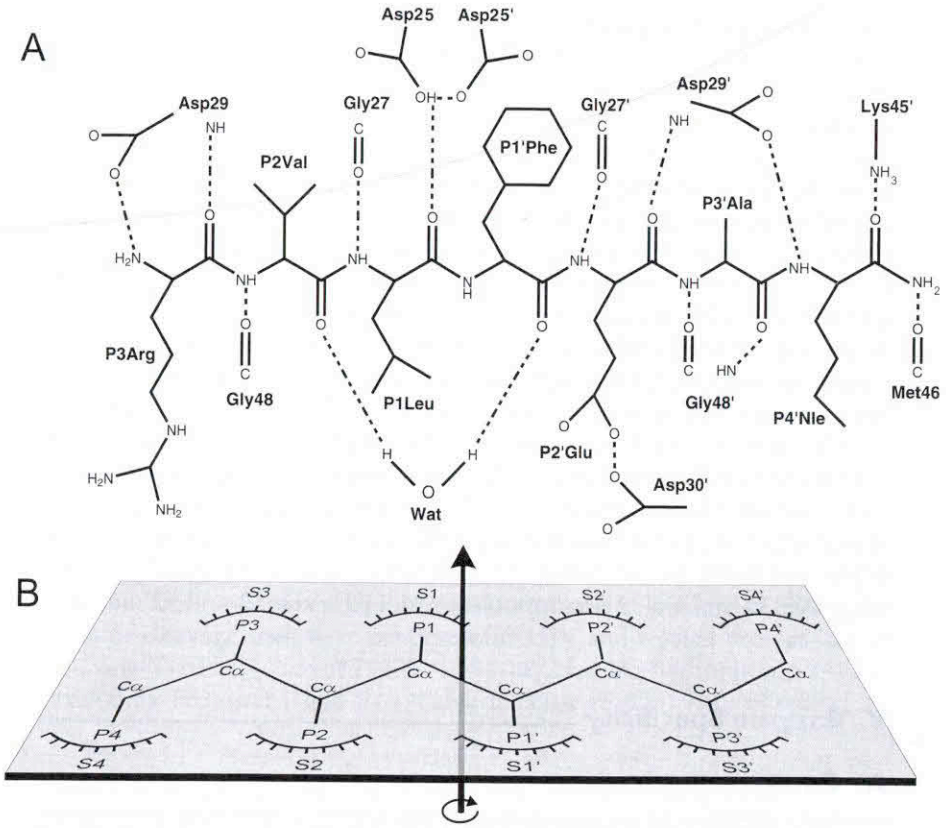

FIGURE 9 Scheme of HIV PR–inhibitor interactions. (A) Hydrogen bond interactions between PR residues and the CA↓p2 substrate analog as deduced from the crystal structures (Weber *et al.*, 1997; Wu *et al.*, 1998). Only the PR residues that form hydrogen bond interactions with the peptide are shown. The substrate residues P3–P4′ are shown. Dashed lines indicate hydrogen bonds. Residues in the second subunit of the PR dimer are indicated with a prime. Asp 25 and Asp 25′ are the catalytic aspartates; Asp 25 is protonated in this scheme. The PR hydrogen bond interactions with the substrate main-chain amide and carbonyl oxygen atoms are conserved in different PR–inhibitor crystal structures (Gustchina *et al.*, 1994). The water molecule shown interacting with the carbonyl oxygens of P2 and P1′ is conserved and also interacts with the amides of Ile 50 and Ile 50′. The PR interactions with substrate side chains will depend on the particular substrate sequence. The CA↓p2 peptide shows an interaction between the carboxylates of P2′ Glu and Asp 30′ of the PR. This interaction is expected to involve a proton on either of the acidic groups. (B) Substrate side chains P4–P4′ shown in PR subsites S4–S4′ are indicated by semicircles. This view is approximately perpendicular to the plane of the hydrogen bonds shown in A. The approximate twofold symmetry axis relating the two subunits of the PR dimer is shown.

Analysis of the interactions between HIV PR and peptidic inhibitors showed two major components: (1) Conserved hydrogen bond interactions between the peptidelike NH and C=O groups of the inhibitor and PR residues that are largely independent of the sequence (Fig. 9). The amide

and carboxylate oxygen of Asp29, the carbonyl oxygen of Gly27, and the amide and carbonyl of Gly48 form conserved hydrogen bond interactions with the amides and carbonyl oxygens of the substrate or inhibitor in both subunits. Interactions between the Ile50 amide in both flaps and the carbonyl oxygen of P2 and P1′ are mediated by a conserved water molecule. The main-chain atoms of the peptidic inhibitors were predicted to make a larger contribution than the side-chain groups to the total binding energy (Gustchina *et al.*, 1994). (2) Each amino acid side chain of the inhibitor (P4 to P3′ form a minimum recognition site) fits into successive subsites (S4 to S3′) formed by PR residues (Fig. 9). This interaction depends on the nature of the side-chain group at each position of the peptidic inhibitor and is largely hydrophobic. However, polar groups may form specific hydrogen bond or ionic interactions, as observed for P2′ Glu in the crystal structure of HIV PR with the CA-p2 analog inhibitor (Weber *et al.*, 1997). The major determinants of PR specificity are located within the subsites, as deduced by mutational and kinetic analysis of HIV-1 and Rous Sarcoma virus proteases (Cameron *et al.*, 1993; Grinde *et al.*, 1992; Cameron *et al.*, 1994). Residues Gly48 and Val82 are critical for substrate selection in the S1 and S1′ subsites, while Asp30 and Val32 are important residues in the S2 and S2′ subsites.

V. Enzyme Specificity

A. Catalytic Mechanism

The catalytic mechanism of HIV-1 PR (Hyland *et al.*, 1991) is similar to the "push–pull" mechanism of cellular aspartic proteases proposed by Polgár (1987). The two catalytic Asp 25 residues are structurally adjacent in the dimer with 2.5–3.0 Å separating the closest carboxylate oxygen atoms of each residue, suggesting that one Asp 25 is protonated. The two catalytic aspartates mediate a pH-dependent proton transfer from the attacking water molecule to the leaving nitrogen atom of the substrate. The reaction proceeds through a tetrahedral intermediate and involves a physical step (likely the closing down of the flaps on the substrate molecules) as well as chemical steps (the proton transfer). Interestingly, the rate-limiting step is dependent on the amino acid sequence of the substrate (Polgár *et al.*, 1994). Unlike the serine and cysteine proteinases, which form a covalent acyl-enzyme intermediate with the substrate, aspartyl proteinases do not form a covalent intermediate, and therefore they must rely on multiple anchoring of the substrate to the enzyme on both sides of the scissile bond as shown in Fig. 9. Besides the need for correct catalysis, the extended binding site of retroviral proteases may have an evolutionary advantage. These RNA viruses mutate frequently due to the lack of an editing feature of the RT. Since the enzyme recognizes about seven residues, changes in one or in a few binding subsites

of the enzyme due to mutations may alter, but do not necessarily abolish the enzyme activity or consequently the viral replication.

B. Viral Substrates

The major functional role of the HIV-1 PR is the processing of the viral Gag and Gag-Pol polyproteins in the late phase of replication by catalyzing the hydrolysis of specific peptide bonds in the cleavage sites indicated in Fig. 1. The analysis of naturally occurring cleavage sites, which can be considered as evolutionarily optimized sequences, suggests preferences for certain amino acids at the site of cleavage and in its vicinity (Table I). At P1 and P1′ positions on either side of the cleaved bond hydrophobic amino acids predominate, but Val and Ile are not observed. The occurrence of amino acids at the P1′ position is similar to that found in P1, with the exception that Pro frequently appears in the P1′ position. The P1′ Pro is unique for retroviral PR substrates. No other endopeptidase, except pepsin, is known to hydrolyze cleavage at the imino side of proline. The P2 and P2′ positions are occupied either by hydrophobic or small polar residues, while various types of residues are found at the outer positions. Two major types of cleavage sites were proposed for HIV and related proteases, type 1 having-Tyr(Phe)↓Pro- at P1-P1′ and type 2 having hydrophobic residues (excluding Pro) at P1 and P1′ (Table I; Pettit *et al.*, 1991; Tözsér *et al.*,

TABLE I Protease Cleavage Sites in HIV-1 Gag and Gag-Pol Polyproteins

Location of the cleavage site[a]	*P4*	*P3*	*P2*	*P1*	*P1′*	*P2′*	*P3′*	*Type*[b]
In Gag								
MA↓CA	Ser	Gln	Asn	Tyr	Pro	Ile	Val	1
CA↓p2	Ala	Arg	Val	Leu	Ala	Glu	Ala	2
p2↓NC	Ala	Thr	Ile	Met	Met	Gln	Arg	2
NC↓p1	Arg	Gln	Ala	Asn	Phe	Leu	Gly	(2)
p1↓p6	Pro	Gln	Asn	Phe	Leu	Gln	Ser	(2)
in p6	Lys	Glu	Leu	Tyr	Pro	Leu	Thr	1
In Pol								
TFP↓$p6^{pol}$	Asp	Leu	Ala	Phe	Leu	Gln	Gly	(2)
$p6^{pol}$↓PR	Ser	Phe	Asn	Phe	Pro	Gln	Ile	1
PR↓RT	Thr	Leu	Asn	Phe	Pro	Ile	Ser	1
p66↓p51	Ala	Glu	Thr	Phe	Tyr	Val	Asp	(2)
RT↓IN	Arg	Lys	Ile	Leu	Phe	Leu	Asp	(2)

[a] Notations are according to Schecter and Berger (1967).

[b] Classification of cleavage sites was originally done by Henderson *et al.* (1998) and later modified (Pettit *et al.*, 1991; Tözsér *et al.*, 1992; Griffiths *et al.*, 1992). Oligopeptides corresponding to these cleavage sites were correctly hydrolyzed by the mature PR (Darke *et al.*, 1988; Tözsér *et al.*, 1991; our unpublished results).

1992, Griffiths *et al.*, 1992). These two types of cleavage sites were proposed to have different preferences for the P2 and P2′ positions, and these preferences were later confirmed by enzyme kinetics using oligopeptide substrates.

Other viral proteins were later found to be substrates of the HIV-1 PR. Besides its role in the late phase, it was suggested by experiments with equine infectious anemia virus that the viral PR was required in the early phase of viral replication for cleaving the nucleocapsid protein (Roberts *et al.*, 1991). Subsequently, the nucleocapsid of HIV-1 was confirmed to be a substrate of HIV-1 PR (Wondrak *et al.*, 1994). The accessory protein Nef was also found to be a substrate (Freund *et al.*, 1994). However, the significance of any role of the PR in the early stage is not fully understood.

C. Subsite Preference/Substrate Specificity

The extended substrate binding site of HIV-1 consists of six or seven subsites, based on analysis of the crystal structures of enzyme inhibitor complexes (Fig. 9). The extended binding site was also revealed by studies with oligopeptide substrates where a minimal substrate size of six to seven residues was required for optimal catalysis (Darke *et al.*, 1988; Moore *et al.*, 1989; Billich *et al.*, 1988; Tözsér *et al.*, 1991b). The substrate specificity of the HIV-1 PR has been characterized by using either polyproteins or oligopeptides as substrates (for reviews see Dunn *et al.*, 1994; Tomasselli and Heinrickson, 1994). The results are summerized here. The PR cannot hydrolyze oligopeptides with β-branched amino acids substituted in the P1 position (Phylip *et al.*, 1990). Furthermore, introduction of Pro, Ser, and Gly into P1 also prevented hydrolysis (Tözsér *et al.*, 1992; Cameron *et al.*, 1993). Positively charged (Arg) and negatively charged (Glu) amino acids at P1 or P1′ positions are also not preferred in substrates (Konvalinka *et al.*, 1990; Cameron *et al.*, 1993). Studies with type 1 oligopeptide substrates indicated a preference at P2 for small residues like Cys or Asn (which is also one of the most frequent amino acid at this position in the polyprotein) and preference for β-branched Val or Ile at P2′ position for HIV-1 PR (Margolin *et al.*, 1990, Tözsér *et al.*, 1992). On the other hand, studies of type 2 substrates showed that β-branched residues, especially Val, were favorable at P2, while Glu was preferred at P2′ (Phylip *et al.*, 1990; Griffiths *et al.*, 1992). Interestingly, Glu was found to be preferred at P2′ in a peptide series in which the P2-P1′ sequence of a type 1 cleavage site (-Asn-Tyr ↓ Pro-) was introduced into a type 2 substrate. Therefore, a general preference for P2′ Glu by the HIV-1 PR was suggested (Griffiths *et al.*, 1992). However, P2′ Glu was found to be unfavorable in another type 2 series based on a palindromic sequence having two tyrosines at the site of cleavage (Tözsér *et al.*, 1997b). In good agreement with the naturally occurring cleavage site sequences, various residues were acceptable by the S3 and S4′ subsites of HIV-1 (Konvalinka *et al.*, 1990, Tözsér *et al.*, 1992; Cameron *et al.*, 1993),

while smaller residues were preferred at P4 (Tözsér *et al.*, 1991b). In summary, HIV PR shows a preference for large hydrophobic residues at P1 and P1′, smaller hydrophobic residues at P2, and accommodates a variety of residues at P3 and P3′, while the P2′ preference depends on the peptide sequence.

The different preferences for P2 and P2′ residues as a function of the residues present at P1 and P1′ suggested that the preference for the amino acid at certain positions might strongly depend on the sequence context and conformation of the peptide substrate. The sequence context dependence of the HIV-1 PR was studied for the whole substrate by using doubly and multiply substituted peptides (Ridky *et al.*, 1996; Tözsér *et al.*, 1997b). This structural dependence of the substrate specificity arises from the extended conformation of the bound substrate, as deduced from the crystal structures of PR with peptidelike inhibitors (Fig. 9). The specificity depends on the type of amino acid present in neighboring positions in the sequence (i.e., P2 and P1 or P1 and P1′) as well as amino acid side chains that are adjacent in the extended peptide structure (e.g., the side chain of P2 is next to the side chain of P1′, and P1 is next to P2′). The context dependence may substantially contribute to the high specificity of the retroviral proteases, although this is not apparent from the amino acid sequences of the naturally occurring cleavage sites (Table I). Understanding the strong sequence context dependence of the HIV PR substrates has important implications for both the development of drug resistance and the design of new drugs. Mutation of a PR residue in one subsite will directly influence inhibitor and substrate binding at that subsite and can also indirectly influence the specificity of the other subsites. Conversely, changing substrate residues (or inhibitors) at positions other than those which directly interact with the mutated PR subsite can complement the initial change and restore the efficient substrate processing (or the high potency of the inhibitor).

D. Verification of Knowledge of Specificity

Our understanding of the PR specificity has been verified by engineering Rous sarcoma virus (RSV) PR to recognize the substrates and inhibitors of HIV-1 PR. The wild-type RSV PR and the almost-identical avian myeloblastosis virus (AMV) PR do not hydrolyze most peptides representing the HIV-1 cleavage sites and exhibit low affinity for inhibitors of HIV-1 PR (Ridky *et al.*, 1996; Wu *et al.*, 1998). The crystal structures of RSV and HIV-1 proteases show differences in the substrate binding residues and in the length of the flaps. Differences in substrate selection have been correlated with the differences in 9–10 substrate-binding residues of the two proteases (Cameron *et al.*, 1993; Tözsér *et al.*, 1996). The structurally equivalent residues of HIV-1 PR were substituted into RSV PR. The individual mutations increase the catalytic rate (Thr38→Ser and Ser107→Asn) or alter the

substrate specificity (Ile42→Asp, Ile44→Val, Arg105→Pro, Gly106→Val) relative to the wild-type RSV PR (Cameron *et al.*, 1994). The RSV S9 PR designed with nine substitutions of HIV-1 PR residues, Thr38→Ser, Ile42→Asp, Ile44→Val, Met73→Val, Ala100→Leu, Val104→Thr, Arg105→Pro, Gly106→Val, and Ser107→Asn, was shown to hydrolyze all tested substrates of HIV-1 PR and has high affinity for HIV PR inhibitors (Ridky *et al.*, 1996; Wu *et al.*, 1998). The inhibition constants for the CA-p2 analog inhibitor are very similar for RSV S9 and HIV-1 proteases at 20 and 14 n*M*, respectively.

Crystal structures have been determined for both the RSV S9 and HIV-1 proteases with the HIV-1 CA-p2 analog inhibitor (Wu *et al.*, 1998). The RSV S9 interactions with the inhibitor are very similar to those of HIV-1 PR, with the exception of interactions of the flap residues Asn 61, Gln63, and His65 with the distal P3 and P4′ positions of the inhibitor. These interactions of the RSV PR flap residues partially substitute for those of Lys45 and Met46 in the flaps of HIV PR (Fig. 9). This comparison suggests that the interactions of P2-P3′ of the inhibitor with the PR are most important for affinity since the inhibition constants are very similar for RSV S9 and HIV-1 proteases despite the differences in the flap residues. The engineered RSV S9 PR verifies our knowledge of the critical residues for PR recognition of substrates and inhibitors. The key residues Asp30, Val32, Pro81, and Val82 are mutated in drug-resistant HIV-1 PR, as predicted (Cameron *et al.*, 1993).

E. pH-Dependent Processing of the Gag CA-p2 Cleavage Site

The CA↓p2 cleavage site in the HIV-1 Gag precursor is unique in having a conserved Glu at the P2′ position (Table I; Barrie *et al.*, 1996). Cleavage of the CA↓p2 site was shown to be an important regulatory step for the sequential processing of the Gag precursor (Pettit *et al.*, 1994). The CA↓p2 cleavage is also negatively influenced by the p2 domain and is accelerated at low pH. In order to understand the molecular basis for this critical processing step, the crystal structure of HIV-1 PR with a reduced peptide analog of the CA↓p2 site was determined (Weber *et al.*, 1997; Wu *et al.*, 1998). This structure showed a novel proton-mediated interaction between the carboxylates of P2′ Glu and Asp30 of the PR (Fig. 9). The proton-mediated interaction was also observed in the crystal structure of a mutant RSV PR with specificity engineered to bind to the same substrate analog (Wu *et al.*, 1998) and for HIV-2 PR crystallized with a different inhibitor containing P2′ Glu (Tong *et al.*, 1993). Similar interactions between P2′ Glu and Asp30 also occur in the crystal structures of the drug-resistant PR mutants R8Q, K45I, and L90M (see below; Mahalingam *et al.*, 1999); the complex of TFP; the N terminus of the transframe region of Gag-Pol with the HIV-1 PR (Louis *et al.*, 1998); and the product complex with the SIV

PR (Rose *et al.*, 1996). The conservation of the P2′ Glu at the CA ↓ p2 site and its conserved interaction with Asp30 suggest that pH-dependent processing through protonation of P2′ Glu or Asp30 may be a critical regulatory mechanism for PR-mediated protein processing and particle maturation. Consistent with the above observations, the HIV-1 Vpr tethered to the CA-p2 peptide gave nearly complete inhibition of viral replication, unlike the chimera with other peptide substrates (Serio *et al.*, 1997). Also substituting P2′ Glu with Gln of a related chromogenic substrate reduced the catalytic efficiency by ~40-fold at pH 4.0 (Polgar *et al.*, 1994). In accordance with this result, the D30N mutation substantially decreased the replicative capacity of the virus *in vivo* relative to the wild type (Martinez-Picado *et al.*, 1999).

F. Nonviral Substrates

A number of nonviral proteins have been shown to be substrates of HIV-1 PR (for review see Tomasselli and Heinrickson, 1994). One of the first reported nonviral protein substrates of HIV-1 PR was LysPE40, a recombinant derivative of the *Pseudomonas* exotoxin (Tomasselli *et al.*, 1990). However, this protein was hydrolyzed at two unexpected sites and not at the predicted Tyr↓Pro site of the flexible arm of the two domains (Tomasselli *et al.*, 1990). Later, several other nonviral protein substrates of HIV-1 PR were identified, including calmodulin, G-actin, troponin C, prointerleukin 1beta, and lactate dehydrogenase (Tomasselli and Heinrickson, 1994). The intermediate filament proteins vimentin, desmosin, and glial fibrillary acidic protein were found to be cleaved *in vitro* by HIV-1 PR, and microinjection of the enzyme into the cells resulted in the collapse of the vimentin intermediate filament network (Shoeman *et al.*, 1990). The microtubule-associated proteins were also found to be substrates of HIV-1 PR (Wallin *et al.*, 1990). These results indicate that active HIV-1 PR cleavage of cellular proteins may contribute to the pathogenesis associated with the retroviral infection (Kaplan and Swanstrom, 1991). Studies of the nonviral protein substrates provided new cleavage site sequences for databases of HIV PR substrates (Chou *et al.*, 1996). However, many of these sites were not confirmed *in vitro* using peptide substrates. In contrast to the naturally occurring sequences, it is difficult to accommodate the variety of nonviral substrates within any sequence classification and many of these cleavage sites contain charged amino acids, even at P1 or P1′ (Tomasselli and Heinrickson, 1994). A majority of the nonviral substrates have Glu at P2′ (Chou *et al.*, 1996), although only 1 of the 11 HIV-1 polyprotein cleavage sites has P2′ Glu (Table I). Therefore, the HIV-1 PR specificity for nonviral protein substrates appears to differ from its specificity for the viral substrates.

VI. Drug Resistance

Drug resistance is a serious problem for treatment of AIDS infection. Inhibitors of HIV PR are very potent antiviral agents, and several have been

approved for treatment of AIDS. The development of antiviral PR inhibitors is a major success of structure-based drug design (Wlodawer and Vondrasek, 1998). The combination therapy using PR inhibitors as well as inhibitors of the reverse transcriptase has had a great impact in extending the lifetime of AIDS patients (Palella *et al.*, 1998). However, the rapid emergence of drug-resistant HIV poses a severe problem for continuous use of PR inhibitors (Korant and Rizzo, 1997). Moreover, multidrug resistance has been observed recently in patients on a combination therapy of RT and PR inhibitors (Shafer *et al.*, 1998). Drug-resistant viruses are selected rapidly due to the high degree of genetic heterogeneity in HIV. The sequence diversity arises due to the error-prone HIV RT (Ji and Loeb, 1992) as well as the high replicative capacity of the virus (Ho *et al.*, 1995; Wei *et al.*, 1995). The RT lacks a 3′-5′-exonuclease proofreading function and has an error rate of ~1 in 10^4. In a fully infected patient as many as 10^9 virus particles are produced daily. Therefore, HIV mutates rapidly.

A. Location of Drug-Resistance Mutations

Resistance to PR inhibitors arises from the selection of mutations in the PR gene (Schinazi *et al.*, 1997). More than 40 mutations have been found in the PR gene of drug-resistant HIV that alter 28 different PR residues (Fig. 2, Table II). Multiple mutations in the PR accumulate over time in response to inhibitor therapy (Molla *et al.*, 1996). In addition, compensating mutations can occur in the PR cleavage sites (Doyon *et al.*, 1996; Zhang *et al.*, 1997). Moreover, the PR gene has extensive natural polymorphisms even in the absence of inhibitors, and these polymorphisms include many amino acid substitutions that contribute to inhibitor resistance (Kozal *et al.*, 1996). Therefore, it is important to understand the molecular basis for drug resistance and to continue the development of new PR inhibitors to overcome the problem of drug resistance.

Mutations are less likely to occur in residues that are essential for the catalytic mechanism, dimer formation, and binding of protein substrates (Table II). About 70% of drug-resistant mutations (Schinazi *et al.*, 1997) and the majority of natural polymorphisms (Kozal *et al.*, 1996) occur in less conserved regions of the PR. The sites of these resistant mutations mapped onto the PR structure are shown in Fig. 2. Many mutations alter residues in the inhibitor binding site and probably act by directly altering the PR affinity for the inhibitor. These include the mutations of V82 arising from exposure to ritonavir or indinavir, Gly48→Val from saquinavir, and Asp30→Asn from nelfinavir. Drug-resistant mutations of these residues were originally predicted on the basis of substrate-specificity studies (Cameron *et al.*, 1993). Other mutations alter residues at the dimer interface, such as Arg8, Ile50, and Leu97; these mutations may exert an effect on dimer formation. Unexpectedly, the majority of resistant mutations alter residues

TABLE II Conserved Regions of HIV-1 Protease and Sites of Drug Resistant Mutations[a]

								K		IRV										R				V									
Mutants								Q		F										M			I	I						N		I	F
								*															*		*		*		*	*		*	
Wild type	P	Q	I	T	L	W	Q	R	P	L	V	T	I	R	I	G	G	Q	L	K	E	A	L	L	D	T	G	A	D	D	T	V	L
	1									10										20										30			
	Interface							Interface														Active site/interface											

													FLV								M												
Mutants			I									I	I	V	V		V				V						E			P			
												*	*	*	*	*	*	*					*										
Wild type	E	E	M	N	L	P	G	K	W	K	P	K	M	I	G	G	I	G	G	F	I	K	V	R	Q	Y	D	Q	I	L	V	E	I
							40										50										60						
															Flap/interface																		

					T											TFIS		A				S											
Mutants					V		S		I		I				T	A		V				D		M			L				V		
										*				*	*	*		*			*												
Wild type	C	G	H	K	A	I	G	T	V	L	V	G	P	T	P	V	N	I	I	G	R	N	L	L	T	Q	I	G	C	T	L	N	F
				70										80										90									99
																		Helix/interface										Interface					

[a] The conserved (–) active site, flap, helix, interface regions of the dimer and residues that are involved in substrate binding (*) are indicated. Protease mutants that are selected upon drug treatment are shown (Schinazi *et al.*, 1997).

that are not part of the inhibitor binding site or the dimer interface. This category includes Leu90→Met and Asn88→Asp, which commonly arise from exposure to saquinavir or nelfinavir, respectively. The molecular basis for the resistance of these distally located mutations is not fully understood.

B. Mutants Exhibit Altered Kinetic Parameters

Resistant PR mutants must act by lowering the PR affinity for the drug while maintaining sufficient catalytic activity for optimal processing of the Gag and Gag-Pol polyproteins leading to the production of infective virions. In order to understand the molecular mechanisms for development of drug resistance, several groups have studied different inhibitor resistant mutants of PR. Most studies have used mutants that were selected by the particular drug of interest and assayed for inhibition and PR activity on a single substrate (Gulnik *et al.*, 1995; Tisdale *et al.*, 1995; Molla *et al.*, 1996). One study has probed the substrate selectivity of mutants Arg8→Lys, Val32→Ile, Val82→Thr, Ile84→Val, Gly48→Val/Leu90→Met, and Val82→Thr/Ile84→Val using a set of peptides based on the HIV-1 CA-p2 cleavage site (Ridky *et al.*, 1998). Recently, a broader range of mutants, Arg8→Gln, Asp30→Asn, Lys45→Ile, Met46→Leu, Gly48→Val, Val82→Ser, Asn88→Asp, and Leu90→Met, were investigated for the hydrolysis of three critical cleavage site peptides and their structural stability (Mahalingam *et al.*, 1999). These studies demonstrate that drug-resistant mutants show alterations in several molecular and enzymatic properties that include lower affinity for inhibitor, altered catalytic rate, substrate specificity, and structural stability.

1. Mutants Exhibit Lower Affinity for Inhibitor

Several studies have shown that when a mutant is selected against a particular inhibitor, the affinity for that inhibitor is reduced (for example, Gulnik *et al.*, 1995; Tisdale *et al.*, 1995; Molla *et al.*, 1996). Cross-resistance has also been observed among different inhibitors. The pattern of mutations and the emergence of cross-resistance are complex and unpredictable (Boden and Markowitz, 1998). A different pattern of mutations is selected by different inhibitors. Exposure to indinavir or ritonavir selects for mutations of Val82 initially, followed by mutations of a number of other residues. In contrast, the single resistant mutations Gly48→Val or Leu90→Met arise from exposure to saquinavir, while Asp30→Asn or Asn88→Asp are commonly selected by nelfinavir (Schinazi *et al.*, 1997).

Many of the individual drug-resistant mutations in the inhibitor binding site have been shown to be critical for substrate specificity. Gly48 and Val82 are important for recognition of the P1 and P1′ amino acid side chains and Asp30 and Val32 are critical for recognition of the amino acids at P2 and P2′ (Cameron *et al.*, 1994; Lin *et al.*, 1995). These mutations are expected to directly alter the PR affinity for substrates and inhibitors. However, two

other common resistant mutations, Leu90→Met and Asp88→Asp, are not part of the substrate or inhibitor binding site, and they must exert an indirect effect on the inhibitor. Crystal structures of PR–inhibitor complexes show few differences from the wild type for the mutants that alter inhibitor binding residues. Direct interactions, mostly changes in van der Waals interactions between the PR and the inhibitor, appear to be responsible for the lowered affinity for the inhibitor (Pazhanisamy *et al.*, 1996; Ala *et al.*, 1997). This analysis again raises the question of how the mutations in regions distant from the binding site cause resistance.

2. *Mutants Exhibit Altered Catalytic Activity and Substrate Specificity*

Resistant mutants show defects in polyprotein processing and decreased replicative capacity (Zennou *et al.*, 1998; Martinez-Picado *et al.*, 1999). The defects in maturation arise from altered catalytic efficiency for substrate hydrolysis. Many PR mutants show reduced catalytic activity on tested substrates (Gulnik *et al.*, 1995). However, increased catalytic activity on viral substrates has been observed for some mutants (Ridky *et al.*, 1998; Mahalingam *et al.*, 1999). The catalytic activity of the PR mutants Arg8→Gln, Asp30→Asn, Lys45→Ile, Met46→Leu, Gly48→Val, Val82→Ser, Asn88→Asp, and Leu90→Met was investigated using oligopeptides representing the cleavage sites CA-p2, $p6^{pol}$-PR, and PR-RT, which are critical for viral maturation (Fig. 10; Mahalingam *et al.*, 1999). These PR mutants include the mutations commonly arising from four inhibitors in clinical use, saquinavir (Gly48→Val and Leu90→Met), indinavir (Val82→Ser and Met46→Leu), ritonavir (Val82→Ser), and nelfinavir (Asp30→Asn and Asn88→Asp) (Boden and Markowitz, 1998). Mutant Arg8→Gln was one of the first inhibitor resistant mutants to be reported (Ho *et al.*, 1994). Lys45→Ile is found in combination with Leu10→Phe and Ile84→Val on exposure to XM323 (Schinazi *et al.*, 1997). The mutants Val82→Ser, Gly48→Val, Asn88→Asp, and Leu90→Met showed reduced catalytic activity compared to the wild-type PR (Fig. 10). Mutant Val82→Ser was the least active, with 2–20% of wild-type PR activity. PR mutants Asn88→Asp, Arg8→Gln, and Leu90→Met exhibited activities ranging from 20 to 40% and Gly48→Val from 50 to 80% of the wild-type activity. In contrast, the D30N mutant showed variable activity on different substrates ranging from 10 to 110% of wild-type activity. Mutants Lys45→Ile and Met46→Leu, usually selected in combination with other mutations, showed activities that are similar to (60–110%) or greater than (110–530%) wild type, respectively.

The substrate preference of PR mutants Arg8→Lys, Val32→Ile, Val82→Thr, Ile84→Val, Gly48→Val/Leu90→Met, and Val82→Thr/Ile84→Val was studied using peptides with single amino acid substitutions in the CA-p2 cleavage site (Ridky *et al.*, 1998). These inhibitor-resistant

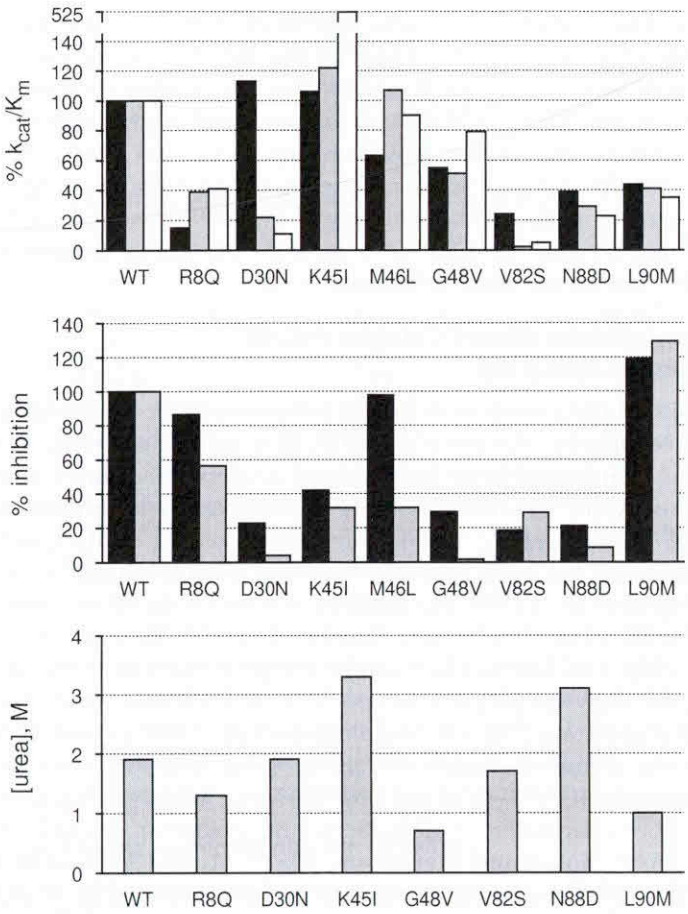

FIGURE 10 Relative inhibition, catalytic efficiency, and structural stability of drug-resistant PR mutants. The PR* and its mutants R8Q, D30N, K45I, G48V, V82S, N88D, and L90M were studied (Mahalingam *et al.*, 1999). The top plot shows the relative k_{cat}/K_m values for hydrolysis of the peptide substrates representing the CA-p2, $p6^{pol}$-PR, and PR-RT cleavage sites. The middle plot shows the relative inhibition for the CA-p2 and p2-NC reduced substrate analog inhibitors. The bottom plot shows the urea concentration at half maximal activity as a measure of structural stability of the mutants relative to the wild type.

mutations were selected because they alter residues in specific subsites of the PR dimer. Residues Val82 and G48 were predicted to be important for the substrate residue binding in S1 and S1′, and Val32 was predicted to be critical for binding in S2 and S2′ (Cameron *et al.*, 1993). Residue 8 contributes to subsites S1, S1′ S3, and S3′, and I84 forms part of S1 and S1′. Surprisingly, these mutants were similar to the wild-type HIV-1 PR in their substrate specificity. Only the Arg8→Lys and Val32→Ile mutants had significant differences from the wild-type PR. The V32I mutant had significantly

enhanced activity on peptides with large hydrophobic residues at P1′, while a smaller enhancement was observed for the Arg8→Lys mutant. This increased preference for large hydrophobic P1′ residues may explain the observed drug-resistant mutation of P1′ Leu to Phe in the Gag p1-p6 cleavage site (Doyon *et al.*, 1996; Zhang *et al.*, 1997). These cleavage site mutations showed improved Gag processing and viral replication in the presence of the drug. Therefore, the altered catalytic rate and altered substrate specificity of the mutant proteases can contribute to drug resistance by enhancing viral replication in the presence of drugs.

C. Mutants Exhibit Altered Structural Stability

Since proper folding and dimer formation are essential for catalytic activity, selected mutants were assayed for their activity as a function of increasing urea concentration. The resistant mutants vary in their structural stability as compared to that of the wild-type PR (Fig. 10; Mahalingam *et al.*, 1999). The mutants Asp30→Asn and Val82→Ser were similar to wild-type PR in their stability toward urea denaturation, while Arg8→Gln, Gly48→Val, and Leu90→Met showed 1.5- to 2.7-fold decreased stability, and Asn88→Asp and Lys45→Ile showed 1.6- to 1.7-fold increased stability. Analysis of the crystal structures of Arg8→Gln, Lys45→Ile, and Leu90→Met mutants complexed with a CA-p2 analog inhibitor showed that the numbers of intersubunit hydrophobic contacts were in good agreement with the relative structural stability of the mutant proteases. The crystal structure of the Arg8→Gln mutant showed changes in the intersubunit interactions as compared to the wild-type PR (Fig. 11). In the wild-type PR, the positively charged side chain of Arg8 forms a strong ionic interaction with the negatively charged side chain of Asp29′ from the other subunit in

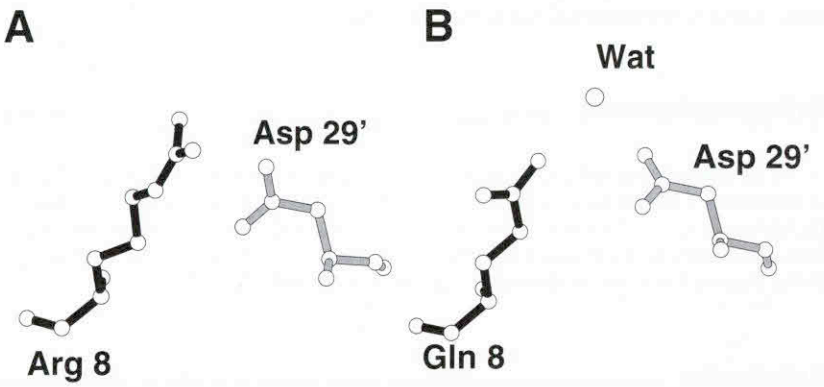

FIGURE 11 The intersubunit interactions of residue 8 in wild-type PR and R8Q mutant. (A) The wild-type ionic interaction of Arg 8 with Asp 29 from the other subunit. (B) The water-mediated hydrogen bond interaction of Gln 8 and Asp 29′ in the R8Q mutant.

the dimer. The Arg8→Gln mutant formed a weaker water-mediated hydrogen bond interaction between the uncharged side chain of Gln8 and Asp29′, which explained its decreased stability toward urea. Therefore, altered stability of the mutant PR dimers can contribute to drug resistance, since dimer formation is critical for catalytic activity. Both increases and decreases in PR stability were observed relative to that of the wild-type PR. Mutants with decreased stability will show more rapid dissociation of the inhibitor as shown for Gly48→Val and Leu90→Met (Maschera *et al.*, 1996), while mutants with increased stability are likely to show greater catalytic activity even in the presence of inhibitor.

D. Drug Resistance Arise by Multiple Mechanisms

Resistance to PR inhibitors can arise by more than one mechanism. Since no direct relationship was observed between relative catalytic activity, inhibition, and structural stability of the different PR mutants (Fig. 10; Mahalingam *et al.*, 1999), drug resistance can arise from independent changes in any one of these parameters. Prolonged exposure to the drug can result in compensating mutations that act in combination to permit optimal polyprotein processing and replicative capacity in the presence of the PR inhibitor. Selected mutations occurring in PR cleavage sites were shown to also compensate for the reduced activity of the initial mutation in the PR domain, thus giving a growth advantage over the primary PR mutation (Doyon *et al.*, 1996; Zhang *et al.*, 1997). An initial mutation that lowers the affinity for the inhibitor and also lowers the catalytic activity or dimer stability can be combined with additional PR mutations that increase the catalytic activity or dimer stability to confer improved viral replication in the presence of inhibitor. Alternatively, the initial PR mutation can be combined with a mutation in the cleavage sites that restores sufficient catalytic activity for optimal virus maturation.

Acknowledgments

This research was sponsored in part by the Intramural AIDS Targeted Antiviral Program of the Office of the Director of the National Institutes of Health, by the United States Public Health Service Grant AI41380, by the Hungarian Science and Research Fund (OTKA T30092, OTKA T22140), by the Hungarian Ministry of Culture and Education (FKFP 1318/97), and by the Fogarty International Research Collaboration Award (TW01001).

References

al-Janabi, J., Hartsuck, J. A., and Tang, J. (1972). Kinetics and mechanism of pepsinogen activation. *J. Biol. Chem.* **247**, 4628–4632.

Ala, P. J., Huston, E. E., Klabe, R. M., McCabe, D. D., Duke, J. L., Rizzo, C. J., Korant, B. D., DeLoskey, R. J., Lam, P. Y., Hodge, C. N., and Chang, C. H. (1997). Molecular basis of HIV-1 protease drug resistance: Structural analysis of mutant proteases complexed with cyclic urea inhibitors. *Biochemistry* **36,** 1573–1580.

Barrie, K. A., Perez, E. E., Lamers, S. L. *et al.* (1996). Natural variation in HIV-1 protease, Gag p7 and p6, and protease cleavage sites within gag/pol polyproteins: Amino acid substitutions in the absence of protease inhibitors in mothers and children infected by human immunodeficiency virus type 1. *Virology* **219,** 407–416.

Beissinger, M., Paulus, C., Bayer, P., Wolf, H., Rosch, P., and Wagner, R. (1996). Sequence-specific resonance assignments of the 1H-NMR spectra and structural characterization in solution of the HIV-1 transframe protein p6. *Eur. J. Biochem.* **237,** 383–392.

Billich, S., Knoop, M.-T., Hansen, J., Strop, P., Sedlacek, J., Mertz, R., and Moelling, K. (1988). Synthetic peptides as substrates and inhibitors of human immunodeficiency virus-1 protease. *J. Biol. Chem.* **263,** 17905–17908.

Boden, D., and Markowitz, M. (1998). Resistance to human immunodeficiency virus type 1 protease inhibitors. *Antimicrob. Agents Chemother.* **42,** 2775–2783.

Cameron, C. E., Grinde, B., Jacques, P. *et al.* (1993). Comparison of the substrate-binding pockets of the Rous sarcoma virus and human immunodeficiency virus type 1 proteases. *J. Biol. Chem.* **268,** 11711–11720.

Cameron, C. E., Ridky, T. W., Shulenin, S. *et al.* (1994). Mutational analysis of the substrate binding pockets of the Rous sarcoma virus and human immunodeficiency virus-1 proteases. *J. Biol. Chem.* **269,** 11170–11177.

Candotti, D., Chappey, C., Rosenheim, M., M'Pele, P., Huraux, J. M., and Agut, H. (1994). High variability of the gag/pol transframe region among HIV-1 isolates. *C. R. Acad. Sci. III* **317,** 183–189.

Co, E., Koelsch, G., Lin, Y., Ido, E., Hartsuck, J. A., and Tang, J. (1994). Proteolytic processing mechanisms of a miniprecursor of the aspartic protease of human immunodeficiency virus type 1. *Biochemistry* **33,** 1248–1254.

Cherry, E., Liang, C., Rong, L. *et al.* (1998). Characterization of human immunodeficiency virus type-1 (HIV-1) particles that express protease-reverse transcriptase fusion proteins. *J. Mol. Biol.* **284,** 43–56.

Chou, K-C., Tomasselli, A. G., Reardon, I. M., and Heinrikson, R. L. (1996). Predicting human immunodeficiency virus protease cleavage sites in proteins by a discriminant function method. *Proteins* **24,** 51–72.

Copeland, T. D., and Oroszlan, S. (1988). Genetic locus, primary structure, and chemical synthesis of human immunodeficiency virus protease. *Gene Anal. Tech.* **5,** 109–115.

Darke, P. L., Nutt, R. F., Brady, S. F., Garsky, V. M., Ciccarone, T. M., Leu, C.-T., Lumma, P. K., Freidinger, R. M., Veber, D. F., and Sigal, I. S. (1988). HIV-1 protease specificity of peptide cleavage is sufficient for processing of Gag and Pol polyproteins. *Biochem. Biophys. Res. Commun.* **156,** 297–303.

Debouck, C. (1992). The HIV-1 protease as a therapeutic target for AIDS. *AIDS Res. Hum. Retroviruses* **8,** 153–164.

Doyon, L., Croteau, G., Thibeault, D., Poulin, F., Pilote, L., and Lamarre, D. (1996). Second locus involved in human immunodeficiency virus type 1 resistance to protease inhibitors. *J. Virol.* **70,** 3763–3769.

Dunn, B. M., Deyrup, C., Moesching, W. G., Gilbert, W. A., Nolan, R. J., and Trach, M. L. (1978). Inhibition of pepsin by zymogen activation fragments: Spectrum of peptides released from pepsinogen NH2 terminus and solid phase synthesis of two inhibitory peptide sequences. *J. Biol. Chem.* **253,** 7269–7275.

Dunn, B. M., Gustchina, A., Wlodawer, A., and Kay, J. (1994). Subsite preferences of retroviral proteinases. *Methods Enzymol.* **241,** 254–278.

Freund, J., Kellner, R., Konvalinka, J., Wolber, V., Krausslich, H.-G., and Kalbitzer, H. R. (1994). A possible regulation of negative factor (Nef) activity of human immunodeficiency virus type 1 by the viral protease. *Eur. J. Biochem.* **223,** 589–593.

Gorelick, R. J., and Henderson, L. E. (1994). "Human Retroviruses and AIDS: Analyses" (G. Myers, B. Korber, S. Wain-Hobson, K.-T. Jeang, L. Henderson, and G. Pavlakis, Eds.), Part III, pp. 2–5. The Los Alamos National Laboratory, Los Alamos, NM. (http://hiv-web.lanl.gov)

Griffiths, J. T., Phylip, L. H., Konvalinka, J., Strop, P., Gustchina, A., Wlodawer, A., Davenport, R. J., Briggs, R., Dunn, B. M., and Kay, J. (1992). Different requirements for productive interaction between the active site of HIV-1 proteinase and substrates containing hydrophobic*hydrophobic- or- aromatic*Pro-cleavage sites. *Biochemistry* **31,** 5193–5200.

Grinde, B., Cameron, C. E., Leis, J., Weber, I. T., Wlodawer, A., Burstein, H., and Skalka, A. M. (1992). Analysis of substrate interactions of the Rous sarcoma virus wild type and mutant proteases and human immunodeficiency virus-1 protease using a set of systematically altered peptide substrates. *J. Biol. Chem.* **267,** 9491–9498.

Gulnik, S. V., Suvorov, L. I., Liu, B., Yu, B., Anderson, B., Mitsuya, H., and Erickson, J. W. (1995). Kinetic characterization and cross-resistance patterns of HIV-1 protease mutants selected under drug pressure. *Biochemistry* **34,** 9282–9287.

Gustchina, A., and Weber, I. T. (1991). Comparative analysis of the sequences and structures of HIV-1 and HIV-2 proteases. *Proteins* **10,** 325–339.

Gustchina, A., Sansom, C., Prevost, M. *et al.* (1994). Energy calculations and analysis of HIV-1 protease-inhibitor crystal structures. *Protein Eng.* **7,** 309–317.

Hatfield, D. L., Levin, J. G., Rein, A., and Oroszlan, S. (1992). Translational suppression in retroviral gene expression. *Adv. Virus Res.* **41,** 193–239.

Henderson, L. E., Benveniste, R. E., Sowder, R., Copeland, T. D., Schultz, A. M., and Oroszlan, S. (1988). Molecular characterization of *gag* proteins from simian immunodeficiency virus (SIV_{Mne}). *J. Virol.* **62,** 2587–2595.

Henderson, L. E., Bowers, M. A., Sower, R. C., Serabyn, S. A., Johnson, D. G., Bess, J. W., Jr., Arthur, L. O., Bryant, D. K., and Fenselau, C. (1992). Gag proteins of the highly replicative MN strain of human immunodeficiency virus type 1: Posttranslational modifications, proteolytic processings, and complete amino acid sequences. *J. Virol.* **66,** 1856–1865.

Ho, D. D., Neumann, A. U., Perelson, A. S., Chen, W., Leonard, J. M., and Markowitz, M. (1995). Rapid turnover of plasma virions and CD4 lymphocytes in HIV-1 infections. *Nature* **373,** 123–126.

Ho, D. D., Toyoshima, T., Mo, H., Kempf, D. J., Norbeck, D., Chen, C. M., Wideburg, N. E., Burt, S. K., Erickson, J. W., and Singh, M. K. (1994). Characterization of human immunodeficiency virus type 1 variants with increased resistance to a C2-symmetric protease inhibitor. *J. Virol.* **68,** 2016–2020.

Hyland, L. J., Tomaszek, T. A., and Meek, T. D. (1991). Human immunodeficiency virus-1 protease. 2. Use of pH rate studies and solvent isotope effects to elucidate details of chemical mechanism. *Biochemistry* **30,** 8454–8463.

Ido, E., Han, H. P., Kezdy, F. J., and Tang, J. (1991). Kinetic studies of human immunodeficiency virus type 1 protease and its active-site hydrogen bond mutant A28S. *J. Biol. Chem.* **266,** 24359–24366.

Jacks, T., Power, M. D., Masiarz, F. R., and Varmus, H. E. (1988). Characterization of ribosomal frameshifting in HIV-1 *gag-pol* expression. *Nature* **331,** 280–283.

Ji, J. P., and Loeb, L. A. (1992). Fidelity of HIV-1 reverse transcriptase copying RNA *in vitro*. *Biochem.* **31,** 954–958.

Kaplan, A. H., and Swanstrom, R. (1991). Human immunodeficiency virus type 1 Gag proteins are processed in two cellular compartments. *Proc. Natl. Acad. Sci. USA* **88,** 4528–4532.

Kaplan, A. H., Zack, J. A., Knigge, M. *et al.* (1993). Partial inhibition of the human immunodeficiency virus type 1 protease results in aberrant virus assembly and the formation of noninfectious particles. *J. Virol.* **67,** 4050–4055.

Karacostas, V., Wolffe, E. J., Nagashima, K., Gonda, M. A., and Moss, B. (1993). Overexpression of the HIV-1 gag-pol polyprotein results in intracellular activation of HIV-1 protease and inhibition of assembly and budding of virus-like particles. *Virology* **193,** 661–671.

Khan, A. R., and James, M. N. (1998). Molecular mechanisms for the conversion of zymogens to active proteolytic enzymes. *Prot. Sci.* **7**, 815–836.

Konvalinka, J., Strop, P., Velek, J., Cerna, V., Kostka, V., Phylip, L. H., Richards, A. D., Dunn, B. M., and Kay, J. (1990). Sub-site preferences of the aspartic proteinase from the human immunodeficiency virus, HIV-1. *FEBS Lett.* **268**, 35–38.

Korant, B. D., and Rizzo, C. J. (1997). The HIV protease and therapies for AIDS. *Adv. Exp. Med. Biol.* **421**, 279–284.

Kozal, M. J., Shah, N., Shen, N., Yang, R., Fucini, R., Merigan, T. C., Richman, D. D., Morris, D., Hubbell, E., Chee, M., and Gingeras, T. R. (1996). Extensive polymorphisms observed in HIV-1 clade B protease gene using high-density oligonucleotide arrays. *Nature Med.* **2**, 753–759.

Krausslich, H. G. (1991). Human immunodeficiency virus proteinase dimer as component of the viral polyprotein prevents particle assembly and viral infectivity. *Proc. Natl. Acad. Sci. USA* **88**, 3213–3217.

Lam, P. Y., Jadhav, P. K., Eyermann, C. J. *et al.* (1994). Rational design of potent, bioavailable, nonpeptide cyclic ureas as HIV protease inhibitors. *Science* **263**, 380–384.

Leis, J., Baltimore, D., Bishop, J. M. *et al.* (1988). Standardized and simplified nomenclature for proteins common to all retroviruses. *J. Virol.* **62**, 1808–1809.

Lin, Y., Lin, X., Hong, L., Foundling, S., Heinrikson, R. L., Thaisrivongs, S., Leelamanit, W., Raterman, D., Shah, M, Dunn, B. M., and Tang, J. (1995). Effect of point mutations on the kinetics and the inhibition of human immunodeficiency virus type 1 protease: Relationship to drug resistance. *Biochemistry* **34**, 1143–1152.

Louis, J. M., Dyda, F., Nashed, N. T., Kimmel, A. R., and Davies, D. R. (1998). Hydrophilic peptides derived from the transframe region of Gag-Pol inhibit the HIV-1 protease. *Biochemistry* **37**, 2105–2110.

Louis, J. M., McDonald, R. A., Nashed, N. T., *et al.* (1991a). Autoprocessing of the HIV-1 protease using purified wild-type and mutated fusion proteins expressed at high levels in *Escherichia coli*. *Eur. J. Biochem.* **199**, 361–369.

Louis, J. M., Oroszlan, S., and Mora, P. T. (1991b). Studies of the autoprocessing of the HIV-1 protease using cleavage site mutants. *Adv. Exp. Med. Biol.* **306**, 499–502.

Louis, J. M., Smith, C. A., Wondrak, E. M., Mora, P. T., and Oroszlan, S. (1989). Substitution mutations of the highly conserved arginine 87 of HIV-1 protease result in loss of proteolytic activity. *Biochem. Biophys. Res. Commun.* **164**, 30–38.

Louis, J. M., Nashed, N. T., Parris, K. D., Kimmel, A. R., and Jerina, D. M. (1994). Kinetics and mechanism of autoprocessing of human immunodeficiency virus type 1 protease from an analog of the Gag-Pol polyprotein. *Proc. Natl. Acad. Sci. USA* **91**, 7970–7974.

Louis, J. M., Wondrak, E. M., Kimmel, A. R., Wingfield, P. W., and Nashed, N. T. (1999a). Proteolytic processing of the HIV-1 protease precursor: Kinetics and mechanism. *J. Biol. Chem.* **274**, 23437–23442.

Louis, J. M., Clore, G. M., and Gronenborn. (1999b). HIV-1 protease regulation: Autoprocessing is tightly coupled to protein folding. *Nat. Struct. Biol.* **6**, 868–875.

Mahalingam, B., Louis, J. M., Reed, C. C., Adomat, J. M., Krouse, J., Wang, Y-F., Harrison, R. W., and Weber, I. T. (1999). Structural and kinetic analysis of drug resistant variants of HIV-1 protease. *Eur. J. Biochem.* **263**, 238–245.

Maschera, B., Darby, G., Palu, G., Wright, L. L., Tisdale, M., Myers, R., Blair, E. D., and Furfune, E. S. (1996). Human immunodeficiency virus: Mutations in the viral protease that confer resistance to saquinavir increase the dissociation rate constant of the protease–saquinavir complex. *J. Biol. Chem.* **271**, 33231–33235.

Margolin, N., Heath, W., Osborne, E., Lai, M., and Vlahos, C. (1990). Substitutions at the P_2' site of *gag* P17-P24 affect cleavage efficiency by HIV-1 protease. *Biochem Biophys Res Commun.* **167**, 554–560.

Martinez-Picado, J., Savara, A. V., Sutton, L., and D'Aquila, R. T. (1999). Replicative fitness of protease inhibitor-resistant mutants of human immunodeficiency virus type 1. *J. Virol.* **73**, 3744–3752.

Mildner, A. M., Rothrock, D. J., Leone, J. W. *et al.* (1994). The HIV-1 protease as enzyme and substrate: Mutagenesis of autolysis sites and generation of a stable mutant with retained kinetic properties. *Biochemistry* **33**, 9405–9413.

Molla, A., Korneyeva, M., Gao, Q., Vasavanonda, S., Schipper, P. J., Mo, H.-M., Markowitz, M., Chernyavskiy, T., Niu, P., Lyons, N., Hsu, A., Granneman, R., Ho, D. D., Boucherm C. A. B., Leonard, J. M., Norbeck, D. W., and Kempf, D. J. (1996). Ordered accumulation of mutations in HIV protease confers resistance to ritonavir. *Nature Med.* **2**, 760–766.

Moore, M. L., Bryan, W. M., Fakhoury, S. A., Magaard, V. W., Huffman, W. F., Dayton, B. D., Meek, T. D., Hyland, L., Dreyer, G. B., Metcalf, B. W., Strickler, J. E., Gorniak, J. G., and Debouck, C. (1989). Peptide substrates and inhibitors of the HIV-1 protease. *Biochem. Biophys. Res. Commun.* **159**, 420–425.

Oroszlan, S., and Luftig, R. B. (1990). Retroviral proteases. *Curr. Topics Microbiol. Immunol.* **157**, 153–185.

Palellar, F. J., Delaney, K. M., Moorman, A. C., Loveless, M. O., Fuhrer, J., Satten, G. A., Aschman, D. J., and Holmberg, S. D. (1998). Declining morbidity and mortality among patients with advanced human immunodeficiency virus infection. *N. Engl. J. Med.* **338**, 853–860.

Partin, K., Zybarth, G., Ehrlich, L., DeCrombrugghe, M., Wimmer, E., and Carter, C. (1991). Deletion of sequences upstream of the proteinase improves the proteolytic processing of human immunodeficiency virus type 1. *Proc. Natl. Acad. Sci. USA* **88**, 4776–4780.

Pazhanisamy, S., Stuver, C. M., Cullinan, A. B., Margolin, N., Rao, B. G., and Livingston, D. J. (1996). Kinetic characterization of human immunodeficiency virus type-1 protease-resistant variants. *J. Biol. Chem.* **271**, 17979–17985.

Pearl, L. H., and Taylor, W. R. (1987). A structural model for the retroviral proteases. *Nature* **329**, 351–34.

Pettit, S. C., Moody, M. D., Wehbie, R. S. *et al.* (1994). The p2 domain of human immunodeficiency virus type 1 Gag regulates sequential proteolytic processing and is required to produce fully infectious virions. *J. Virol.* **68**, 8017–8027.

Pettit, S. C., Simsic, J., Loeb, D. D., Everitt, L., Hutchinson, C. A., III, and Swanstrom, R. (1991). Analysis of retroviral protease cleavage sites reveals two types of cleavage sites and the structural requirements of the P1 amino acid. *J. Biol. Chem* **266**, 14539–14547.

Phylip, L. H., Richards, A. D., Kay, J., Konvalinka, J., Strop, P., Blaha, I., Velek, J., Kostka, V., Ritchie, A. J., Broadhurst, A. V., Farmerie, W. G., Scarborough, P. E., and Dunn, B. M. (1990). Hydrolysis of synthetic chromogenic substrates by HIV-1 and HIV-2 proteinases. *Biochem. Biophys. Res. Commun.* **171**, 439–444.

Phylip, L. H., Mills, J. S., Parten, B. F., Dunn, B. M., and Kay, J. (1992). Intrinsic activity of precursor forms of HIV-1 proteinase. *FEBS Lett.* **314**, 449–454.

Polgár, L. (1987). The mechanism of action of aspartic proteinases involves "push–pull" catalysis. *FEBS Lett.* **219**, 1–4.

Polgár, L., Szeltner, Z., and Boros, I. (1994). Substrate-dependent mechanisms of the catalysis of human immunodeficiency virus protease. *Biochemistry* **33**, 9351–9357.

Richards, A. D., Kay, J., Dunn, B. M., Bessant, C. M., and Charlton, P. A. (1992). Inhibition of aspartic proteinases by synthetic peptides derived from the propart region of human prorenin. *Int. J. Biochem.* **24**, 297–301.

Ridky, T. W., Cameron, C. E., Cameron, J., Leis, J., Copeland, T. D., Wlodawer, A., Weber, I. T., and Harrison, R. W. (1996). Human immunodeficiency virus, type 1 protease substrate specificity is limited by interactions between substrate amino acids bound in adjacent enzyme subsites. *J. Biol. Chem.* **271**, 4709–4717.

Ridky, T. W., Kikonyogo, A., Leis, J. *et al.* (1998). Drug-resistant HIV-1 proteases identify enzyme residues important for substrate selection and catalytic rate. *Biochemistry* **37**, 13835–13845.

Roberts, M. M., Copeland, T. D., and Oroszlan, S. (1991). *In situ* processing of a retroviral nucleocapsid protein by the viral proteinase. *Prot. Eng.* **4**, 695–700.

Rose, J. R., Babe, L. M., and Craik, C. S. (1995). Defining the level of human immunodeficiency virus type 1 (HIV-1) protease activity required for HIV-1 particle maturation and infectivity. *J. Virol.* **69**, 2751–2758.

Rose, R. B., Craik, C. S., Douglas, N. L., and Stroud, R. M. (1996). Three-dimensional structures of HIV-1 and SIV protease product complexes. *Biochemistry* **35**, 12933–12944.

Rose, J. R., Salto, R., and Craik, C. S. (1993). Regulation of autoproteolysis of the HIV-1 and HIV-2 proteases with engineered amino acid substitutions. *J. Biol. Chem.* **268**, 11939–11945.

Schechter, I., and Berger, A. (1967). On the size of the active site in proteases. I. Papain. *Biochem. Biophys. Res. Commun.* **27**, 157–172.

Schinazi, R. F., Larder, B. A., and Mellors, J. W. (1997). Mutations in retroviral genes associated with drug resistance. *Int. Antivir. News* **5**, 129–142.

Serio, D., Rizvi, T. A., Cartas, M. *et al.* (1997). Development of a novel anti-HIV-1 agent from within: Effect of chimeric Vpr-containing protease cleavage site residues on virus replication. *Proc. Natl. Acad. Sci. USA* **94**, 3346–3351.

Shafer, R. W., Winters, M. A., Palmer, S., and Merigan, T. C. (1998). Multiple concurrent reverse transcriptase and protease mutations and multidrug resistance of HIV-1 isolates from heavily treated patients. *Ann. Intern. Med.* **128**, 906–911.

Shoeman, R. L., Höner, B., Stoller, T. J., Kesselmeier, C., Miedel, M. C., Traub, P., and Graves, M. C. (1990). Human immunodeficiency virus type 1 protease cleaves the intermediate filament proteins vimentin, desmin, and glial fibrillary acidic protein. *Proc. Natl. Acad. Sci. USA* **87**, 6336–6340.

Tessmer, U., and Krausslich, H. G. (1998). Cleavage of human immunodeficiency virus type 1 proteinase from the N- terminally adjacent p6* protein is essential for efficient Gag polyprotein processing and viral infectivity. *J. Virol.* **72**, 3459–3463.

Tisdale, M., Myers, R. E., Maschera, B., Parry, N. R., Oliver, N. M., and Blair, E. D. (1995). Cross-resistance analysis of human immunodeficiency virus type 1 variants individually selected for resistance to five different protease inhibitors. *Antimicrob. Agents Chemother.* **39**, 1704–1710.

Tomasselli, A. G., and Heinrickson, R. L. (1994). Specificity of retroviral proteases: An analysis of viral and nonviral protein substrates. *Methods Enzymol.* **241**, 279–301.

Tomasselli, A. G., Hui, J. O., Sawyer, T. K., Staples, D. J., FitzGerald, D. J., Chaudhary, V. K., Pastan, I., and Heinrikson, R. L. (1990). Interdomain hydrolysis of a truncated *Pseudomonas* exotoxin by the human immunodeficiency virus-1 protease. *J. Biol. Chem.* **265**, 408–413.

Tong, L., Pav, S., Pargellis, C., Do, F., Lamarre, D., and Anderson, P. C. (1993). Crystal structure of human immunodeficiency virus (HIV) type 2 protease in complex with a reduced amide inhibitor and comparison with HIV-1 protease structures. *Proc. Natl. Acad. Sci. USA* **90**, 8387–8391.

Tözsér, J., Bagossi, P., Weber, I. T., Copeland, T. D., and Oroszlan, S. (1996). Comparative studies on the substrate specificity of avian myeloblastosis virus proteinase and lentiviral proteinases. *J. Biol. Chem.* **271**, 6781–6788.

Tözsér, J., Bláha, I., Copeland, T. D., Wondrak, E. M., and Oroszlan, S. (1991a). Comparison of the HIV-1 and HIV-2 proteinases using oligopeptide substrates representing cleavage sites in Gag and Gag-Pol polyproteins. *FEBS Lett.* **281**, 77–80.

Tözsér, J., Gustchina, A., Weber, I. T., Bláha, I., Wondrak, E. M., and Oroszlan, S. (1991b). Studies on the role of the S_4 substrate binding site of HIV proteinases. *FEBS Lett.* **279**, 356–360.

Tözsér, J., Weber, I. T., Gustchina, A., Bláha, I., Copeland, T. D., Louis, J. M., and Oroszlan, S. (1992). Kinetic and modeling studies of S_3-S_3' subsites of HIV proteinases. *Biochemistry* **31**, 4739–4800.

Tözsér, J., Yin, F. H., Cheng, Y. S. *et al.* (1997a). Activity of tethered human immunodeficiency virus 1 protease containing mutations in the flap region of one subunit. *Eur. J. Biochem.* **244**, 235–241.

Tözsér, J., Bagossi, P. Weber, I. T., Louis, J. M., Copeland, T. D., and Oroszlan, S. (1997b). Studies on the symmetry and sequence context dependence of the HIV-1 proteinase specificity. *J. Biol. Chem.* **272**, 16807–16814.

Vogt, V. M. (1996). Proteolytic processing and particle maturation. *Curr. Top. Microbiol. Immunol.* **214**, 95–131.

Wallin, M., Deinum, J., Goobar, L., and Danielson, U. H. (1990). Proteolytic cleavage of microtubule-associated proteins by retroviral proteinases. *J. Gen. Virol.* **71**, 1985–1991.

Weber, I. T. (1990). Comparison of the crystal structures and intersubunit interactions of human immunodeficiency and Rous sarcoma virus proteases. *J. Biol. Chem.* **265**, 10492–10496.

Weber, I. T., Wu, J., Adomat, J. *et al.* (1997). Crystallographic analysis of human immunodeficiency virus 1 protease with an analog of the conserved CA-p2 substrate—Interactions with frequently occurring glutamic acid residue at P2′ position of substrates. *Eur. J. Biochem.* **249**, 523–300.

Wei, X., Goshm S. K., Taylor, M. E., Johnson, V. A., Emini, E. A., Deutsch, P., Lifson, J. D., Bonhoeffer, S., Nowak, M. A., Hahn, B. H. *et al.* (1995). Viral dynamics in human immunodeficiency virus type 1 infection. *Nature* **373**, 117–122.

Wishart, D. S., Bigam, C. G., Holm, A., Hodges, R. S., and Sykes, B. D. (1995). ^{1}H, ^{13}C and ^{15}N random coil NMR chemical shifts of the common amino acids. I. Investigations of nearest-neighbor effects. *J. Biomol. NMR* **5**, 67–81.

Wlodawer, A., and Erickson, J. W. (1993). Structure-based inhibitors of HIV-1 protease. *Ann. Rev. Biochem.* **62**, 543–585.

Wlodawer, A., and Vondrasek, J. (1998). Inhibitors of HIV-1 protease: A major succes of structure-assisted drug design. *Annu. Rev. Biophys. Biomol. Struct.* **27**, 249–284.

Wondrak, E. M., and Louis, J. M. (1996). Influence of flanking sequences on the dimer stability of human immunodeficiency virus type 1 protease. *Biochemistry* **35**, 12957–12962.

Wondrak, E. M., Louis, J. M., de Rocquigny, H., Chermann, J. C., and Roques, B. P. (1993). The gag precursor contains a specific HIV-1 protease cleavage site between the NC (P7) and P1 proteins. *FEBS Lett.* **333**, 21–24.

Wondrak, E. M., Nashed, N. T., Haber, M. T., Jerina, D. M., and Louis, J. M. (1996). A transient precursor of the HIV-1 protease: Isolation, characterization, and kinetics of maturation. *J. Biol. Chem.* **271**, 4477–4481.

Wondrak. E. M., Sakaguchi, K., Rice, W. G., Kun, E., Kimmel, A. R., and Louis, J. M. (1994). Removal of zinc is required for processing of the mature nucleocapsid protein of human immunodeficiency virus, type 1, by the viral protease. *J. Biol. Chem.* **269**, 21948–21950.

Wu, J., Adomat, J. M., Ridky, T. W. *et al.* (1998). Structural basis for specificity of retroviral proteases. *Biochemistry* **37**, 4518–4526.

Yamazaki, T., Nicholson, L. K., Torchia, D. A. *et al.* (1994). Secondary structure and signal assignments of human- immunodeficiency-virus-1 protease complexed to a novel, structure-based inhibitor. *Eur. J. Biochem.* **219**, 707–712.

Zennou, V., Mammano, F., Paulous, S., Mathez, D., and Claval, F. (1998). Loss of viral fitness associated with multiple Gag and Gag-Pol processing defects in human immunodeficiency virus type 1 variants selected for resistance to protease inhibitors *in vivo*. *J. Virol.* **72**, 3300–3306.

Zhang, Y. M., Imamichi, H., Imamichi, T., Lane, H. C., Fallon, J., Vasudevachari, M. B., and Salzman, N. P. (1997). Drug resistance during indinavir therapy is caused by mutations in the protease gene and in its Gag substrate cleavage sites. *J. Virol.* **71**, 6662–6670.

Zybarth, G., and Carter, C. (1995). Domains upstream of the protease (PR) in human immunodeficiency virus type 1 Gag-Pol influence PR autoprocessing. *J. Virol.* **69**, 3878–3884.

Zybarth, G., Krausslich, H. G., Partin, K., and Carter, C. (1994). Proteolytic activity of novel human immunodeficiency virus type 1 proteinase proteins from a precursor with a blocking mutation at the N terminus of the PR domain. *J. Virol.* **68**, 240–250.